UC San Diego

UC San Diego Electronic Theses and Dissertations

Title

The spontaneous neoantigen-specific CD4+ T cell response to a growing tumor is functionally and phenotypically diverse

Permalink

https://escholarship.org/uc/item/4310n3sm

Author

Griswold, Ryan

Publication Date

2024

Peer reviewed|Thesis/dissertation

eScholarship.org Powered by the California Digital Library
University of California

UNIVERSITY OF CALIFORNIA SAN DIEGO

The spontaneous neoantigen-specific CD4$^+$ T cell response to a growing tumor is functionally and phenotypically diverse

A dissertation submitted in partial satisfaction of the requirements

for the degree Doctor of Philosophy

in

Biomedical Sciences

by

Ryan Griswold

Committee in charge:

Professor Li-Fan Lu, Chair

Professor Jack Bui

Professor John Chang

Professor Enfu Hui

Professor Gerald Morris

Professor Stephen Schoenberger

2024

Copyright

Ryan Quinn Griswold, 2024

All rights reserved.

The dissertation of Ryan Griswold is approved, and it is acceptable in quality and form for publication on microfilm and electronically.

University of California San Diego

2024

TABLE OF CONTENTS

Dissertation Approval Page iii

Table of Contents iv

List of Figures vi

List of Tables vii

Acknowledgements viii

Vita ix

Abstract of the Dissertation x

Introduction 1

CHAPTER 1: Defining the role of NeoAg-specific CD4+ T cells in the outgrowth of an aggressive MHC-II-negative squamous cell carcinoma. 12

CHAPTER 2: A complete longitudinal phenotypic characterization of the natural NeoAg-specific CD4+ T cell response throughout progressive tumor growth and in response to therapeutic vaccination. 15

CHAPTER 3: Single-cell transcriptional profiling of NeoAg-specific $CD4^+$ T cells during progressive tumor growth. 18

CHAPTER 4: Functional characterization and therapeutic potential of high- and low-affinity TCRs isolated from natural NeoAg-specific CD4+ T cells. 20

DISCUSSION 22

METHODS 27

References 53

LIST OF FIGURES

Figure 1: The multi-faceted roles of neoantigen-specific $CD4^+$ T cells 33

Figure 2: Tracking the development of neoantigen-specific $CD4^+$ T cells against SCC VII in the tumor-draining lymph node..... 35

Figure 3: Phenotyping the developing $CD4^+$ T cell response against SCC VII in the tumor-draining lymph node 38

Figure 4: Phenotyping tumor-infiltrating $CD4^+$ T cells in SCC VII 40

Figure 5: Investigating the clonality and genetic profile of the neoantigen-specific CD4+ T cell response using single cell genomics 42

Figure 6: Characterizing the clonality and phenotypes of $CLTC_{H129>Q}$-specific TCRs ... 44

Figure 7: Expression and characterization of neoantigen-specific TCRs 46

Supplemental Figure 1: Different activation states for total and $CLTC_{H129>Q}$-specific CD4+ T cells 49

Supplemental Figure 2: Transduction efficiency of adoptively transferred cells 50

LIST OF TABLES

Table 1: List of TCRs of interest 51

Table 2: Ability of each TCR to be expressed and bind tetramer 52

ACKNOWLEDGEMENTS

I would like to acknowledge Professor Stephen Schoenberger for his support as my principal investigator. His experience and guidance were invaluable in shaping this work and my understanding of the immune system as a whole.

I would also like to thank my lab members, especially Spencer Brightman for help in streamlining some of the processes and assisting in troubleshooting, Karla Soria Zavala for assisting me with the technical execution of experiments, and Rukman Thota and Martin Naradikian for developing some of the procedures I used.

Finally, I would like to acknowledge my brother Kyle Griswold as well as my parents Mia and Michael Griswold for their reassuring warmth and support throughout this process.

The bulk of chapter 1 as well as the entirety of chapters 2, 3, and 4 are sourced from a manuscript entitled “The spontaneous neoantigen-specific CD4+ T cell response to a growing tumor is functionally and phenotypically diverse.” currently being submitted for review. As such, I’d like to thank my co-authors Spencer E. Brightman, Karla Soria Zavala, Manuel Azaid Ordaz-Arias, Navid Djassemi, Rukman R. Thota, Martin S. Naradikian, Hannah Dose, Suzie Alarcon, Vijayanand Pandurangan, Bjoern Peters, Arron M Miller, Ezra E. W. Cohen, and Stephen P. Schoenberger.

VITA

2013 Bachelor of Sciences, University of California, Irvine

2017 Master of Science, University of California, Irvine

2024 Doctor of Sciences, University of California San Diego

PUBLICATIONS

FIELDS OF STUDY

Major Field: Biomedical Sciences

Studies in Immunology

Professor Stephen Schoenberger

Professor Li-Fan Lu

ABSTRACT OF THE DISSERTATION

Characterizing the spontaneous neoantigen-specific $CD4^+$ T cell response

by

Ryan Griswold

Doctor of Philosophy in Biomedical Sciences

University of California San Diego, 2024

Professor Li-Fan Lu, Chair

Although the efficacy of many successful immunotherapies is leveraged by T cells specific for neoantigens (NeoAg), non-self-derived antigens expressed by tumors which typically arise from point mutations, the progressive growth of tumors expressing immunogenic mutations suggests that an effective endogenous immune response is avoided or suppressed. $CD4^+$ T cells play critical roles in the regulation of cellular immunity through the myriad subsets they can comprise but little is known about their

development in response to progressive tumor growth, which limits the ability to evaluate therapeutic opportunities and efficacies. I characterized the endogenous NeoAg-specific $CD4^+$ T cell response to a validated clathrin NeoAg ($CLTC_{H129>Q}$) expressed by SCC VII, an aggressively and poorly immunogenic MHC-II-deficient tumor, using flow cytometry and a $CLTC_{H129>Q}$/I-A^k tetramer throughout progressive tumor growth. We find that the natural $CD4^+$ T cell response to a growing tumor is phenotypically and functionally diverse, with distinct subsets including type 1 helper (Th1), T follicular helper (Tfh)-like, and regulatory T cell (Treg) lineages appearing as early as 9 days after tumor inoculation. Therapeutic vaccination substantially alters the relative ratio of these subsets by sharply reducing Treg frequency among $CLTC_{H129>Q}$-specific $CD4^+$ T cells in both the tumor and tumor-draining lymph node (tdLN). Single cell transcriptomic analysis of $CLTC_{H129>Q}$/I-A^k tetramer-binding $CD4^+$ T cells recapitulated and extended the diversity of the response while permitting profiling of discovered TCRs following transduction into $CD4^+$ T cells. TCRs of varying affinity are found within each functional subset and while affinity played no role in phenotypic fate, adoptive cellular therapies (ACT) using Th1 cells transduced with a Treg-associated TCR were still capable of mediating therapy equally well as those found on cells expressing anti-tumor phenotypes. These findings offer an unprecedented insight into the functional diversity of a natural neoantigen-specific $CD4^+$ T cell response and show how immunotherapeutic intervention influences the phenotype, magnitude, and efficacy of the anti-tumor immune response.

INTRODUCTION

The multifaceted avenues through which $CD4^+$ T cells play a role in anti-tumor immunity cover direct recognition of MHC-II-positive tumors, indirectly enhancing the anti-tumor potential of a number of different cell types, and engaging inhibitory pathways to constrain the immune response. This opens the possibility of using immunotherapy to empower anti-tumor $CD4^+$ T cells or reduce the potency of regulatory $CD4^+$ T cell phenotypes. This includes but is not limited to cytokine treatments that condition $CD4^+$ T cells, adoptive cell therapies consisting of activated and differentiated $CD4^+$ T cells, immune checkpoint blockade, and vaccination with antigen through free peptide, mRNA encoding peptides, or antigen-loaded patient dendritic cells (DCs) (Figure 1)[1–3].

Regardless of the role $CD4^+$ T cells play in mediating anti-tumor immunity, they must first be activated by recognition of their cognate antigen. The two main classes of potential tumor targets are NeoAg and tumor-associated antigens (TAA), which are non-mutated self-derived peptides selectively expressed or overexpressed by tumor cells[4]. Though TAA are often more conserved between different patients than the more personalized NeoAg, the endogenous T cell immune response to these is both constrained during thymic selection and therapies attempting to utilize TAA-specific responses must be very careful of off target effects against host cells expressing lower levels of the antigen[5–7].

Neoantigens don’t face these problems. However, attempting to target NeoAg via immunotherapy is not without its own set of drawbacks. The random nature of point mutations means that NeoAg are very rarely shared between patients even before considering whether a patient’s HLA alleles endow them with the ability to present the

mutated peptide. This necessitates personalized neoantigen discovery and testing for each patient and traditionally involves sequencing the patient and a tumor biopsy, using binding algorithms to identify mutated peptides likely able to be presented by the host's MHC molecules, then *in vitro* testing such as an ELISpot to confirm which predicted neoantigens are able to generate an immune response from the patient's T cells[8–10]. While a minority of neoantigens are conserved driver mutations shared between patients, only a very limited number of these so-called public NeoAgs have been discovered or seen during clinical trials[11].

Despite improvements to predictive MHC-I:NeoAg binding algorithms, the variance between different groups remains high and the success rate of predicated $CD8^+$ T cell-reactive NeoAg remains low[12]. The *in silico* prediction of MHC-II-binding neoantigens is even worse due to the promiscuity of MHC-II:NeoAg interactions, the longer groove area, and the larger range of peptide sizes able to bind MHC-II[13–18]. This necessitates the expensive and time-consuming testing that consumes most of the three to five months the entire pipeline currently takes. Further reducing how long this takes will be important in making therapeutic options aiming to leverage neoantigen-specific cells able to compete with other first-line treatments that don't share this significant delay.

Despite the drawbacks to identifying NeoAg and harnessing NeoAg-specific cells with immunotherapies, their potency merits investigation. Natural NeoAg-specific T cells are associated with durable remission in some cancers and are crucial to the success of immunotherapy in many others, including those mediated by immune checkpoint blockade, personalized cancer vaccines, and some adoptive cell therapies[19–25]. Whereas the contribution of NeoAg-specific $CD8^+$ T cells in controlling MHC-I-expressing tumors is

well documented in a growing body of literature, the role of NeoAg-specific $CD4^+$ T cells is less well understood[26–29]. This is likely due in part to the restricted expression of MHC-II which is normally limited to professional antigen-presenting cells (pAPC) such as DCs, B cells, and macrophages (MΦ), but can be either canonically expressed in some tumor types (e.g. B-cell lymphomas) or induced in others (e.g. melanomas)[30]. Though $CD4^+$ T cells may directly recognize and kill MHC-II-positive tumors through the secretion of cytotoxic molecules like granzyme B, IFN-γ and TNF-α[31], recent evidence suggests that MHC-II expression does not necessarily enable a tumor to directly present endogenous NeoAg that can nonetheless access the class II presentation pathway or that $MHCII^+$ tumor cells may not act as de facto APCs even when they load and express MHC-II:NeoAg complexes, potentially due to a lack of costimulatory molecules like CD80 required for proper $CD4^+$ T cell activation[32,33].

Though the lack of MHC-II expression by most tumors and the questionable ability for MHC-II:NeoAg complexes to be expressed partially limits the role of NeoAg-specific $CD4^+$ T cells in directly recognizing and killing tumors, these cells still play a larger role in mediating antitumor immunity. NeoAg-specific $CD4^+$ T cells may recognize their cognate antigen after it is ingested and presented by pAPCs, which allows them to orchestrate a variety of therapeutic benefits in cancer. These include pAPC licensing via CD40:CD40L interactions during antigen presentation which improves the expression and stability of the MHC:antigen complex[34–36]. It also enhances the priming of effector and memory $CD8^+$ T cells by DCs, the acquisition of a tumorcidal phenotype in MΦ, and the induction of class switching and affinity maturation in B cells[37–40]. NeoAg-specific $CD4^+$ T cells can also secrete inflammatory cytokines such as IFN-γ and TNF within the tumor

microenvironment to directly inhibit tumor growth, suppress pro-tumor accessory cells, and inhibit tumor vasculature[41].

Though there are a plethora of pathways through which $CD4^+$ T cells may act in the context of tumor immunity, no single $CD4^+$ T cell is involved in all of them. An individual cell adopts one phenotype from a range of subsets that are each only able to interact with a few arms of the immune response. Depending on the cytokine, costimulatory, and TCR signals present during their initial priming, $CD4^+$ T cells can develop into a range of specialized functional subsets[42–44]. These include Th1 cells which secrete pro-inflammatory cytokines like IFN-γ and TNF-α to promote cellular immunity, Th2 cells which secrete anti-inflammatory cytokines like IL-4 and IL-10 to promote humoral immunity, T-helper 17 (Th17) cells originally theorized to protect against microbes via the secretion of IL-17 and IL-22, and inhibitory subtypes like Tregs and Type 1 regulatory (Tr1) cells which employ coinhibitory molecules like CTLA-4 and PD-1 on their cell surface as well as the secretion of inhibitory cytokines like IL-10 and TGF-ß to constrain the immune system[45–47]. The full extent of the effects these cytokines have is still being discovered but they are known to play a number of roles in controlling differentiation, downstream signaling, and functional capacity for a myriad of different types of immune cells[48–54.]

A more recently discovered subset of $CD4^+$ T cells, T follicular helper (Tfh) cells, are responsible for the activation, differentiation, and maturation of B cells during recognition of their cognate antigen presented by MHC-II on B cells[55]. B cells, like antigen-presenting DCs, need signals from costimulatory molecules and secreted cytokines both derived from $CD4^+$ T cells during TCR:MHC-II interactions. These include

ICOS:ICOS-L and CD40:CD40L as well as IL-21, an important cytokine for B cell maturation[56–58]. An increasing amount of recent and ongoing research looks at the potential of Tfh cells in controlling cancer via anti-tumor antibody production by B cells[59], reducing anti-tumor $CD8^+$ T cell exhaustion via IL-21 secretion[60], and by inducing tertiary lymphoid structures that allow colocalization of immune cells and superior priming within the tumor microenvironment (TME)[61,62]. The full range of roles Tfh cells play as well as potential ways to utilize these during immunotherapy remains to be fully elucidated.

Three main types of immunotherapies attempt to leverage NeoAg-specific $CD4^+$ T cells to bolster the anti-tumor phenotypes and/or restrain the immune suppressive phenotypes. These are immune checkpoint blockade (ICB), neoantigen vaccination, and adoptive cell therapies.

Immune checkpoint blockade utilizes the administration of antibodies that bind coinhibitory receptors to block their endogenous interactions, which removes constraints on the immune system and endows it with superior anti-tumor potential. They're currently being tested as a first-line treatment for many types of cancer, including breast, cervical, head and neck, lung, rectal, and many more[63]. These have historically targeted CTLA-4, PD-1, and PD-L1, but ongoing clinical trials have begun to target other molecules like LAG-3[64]. Studies are additionally beginning to show the potential of targeting other receptors like TIGIT, Tim-3, IDO, CD39, ICOS, OX40, and 4-1BB[65–73]. There is a fine line between removing the breaks from the anti-tumor immune response and allowing the immune system to attack the host, which necessitates careful dosing and monitoring[74–76].

While ICB does not explicitly target NeoAg-specific immune cells, studies show that tumor mutational burden correlates with the response to ICB[77,78] and more recent studies suggest NeoAg-specific $CD4^+$ and $CD8^+$ T cells are specifically leveraged to attain therapeutic results[79–83]. Ongoing work attempts to understand the differing effects of αPD-1, αCTLA-4, and combining the two. αPD-1 primarily reduces terminal differentiation of $CD8^+$ and $CD4^+$ T cells into states that are less able to proliferate and thus can't sustain anti-tumor activity while αCTLA-4 reduces the frequency and potency of Tregs, which in turn improves DC function and the cytotoxic function of $CD8^+$ T cells[84–93]. There is some disagreement about the ability of αCTLA-4 to deplete Tregs in some human cancers, further emphasizing the complexity of using immunotherapies to tackle different types of tumors[94]. These treatments are far from infallible and work continues to investigate biomarkers able to be used to gauge the efficacy of ongoing ICB regiments[95,96] and to study the state of neoantigen-specific T cells in cancers resistant to ICB in the hope that different combinations of targets or the inclusion of other therapies could improve clinical outcomes[97–99].

Neoantigen vaccination consist of the mutated peptide packed as either free peptide, bound to some targeting molecule like an antibody, or pulsed onto an APC. They're frequently combined with an adjuvant to enhance the response to it. The vaccination specifically aims to enhance the host's endogenous anti-tumor immune response, which either failed to be properly activated or was insufficient to overcome the tumor's immunosuppressive environment during the natural response[100–102]. Though initial neoantigen vaccines primarily or solely targeted $CD8^+$ T cell-reactive neoantigens,

recent studies have emphasized the need to target and additionally include CD4 T cell-reactive epitopes to achieve optimal results even against MHC-II-negative tumors[103,104].

A recent study investigating the optimal formulation of the vaccine suggests the importance of conjoining a $CD4^+$ T cell-reactive epitope to a $CD8^+$ T cell-reactive epitope in attaining the best results, likely because this allows a single dendritic cell that intakes the peptide to present both epitopes thus be licensed by $CD4^+$ T cells to better prime $CD8^+$ T cells[105]. Another study found that it did not matter if the $CD4^+$ T cell-reactive epitope was a neoantigen or a universal helper epitope, which is consistent with prior studies showing conjoined universal helper epitopes improved the CD8 response in nontumor vaccinations[106,107]. Given the robust roles of NeoAg-specific $CD4^+$ T cells and the potential for off target effects of universally activated $CD4^+$ T cells, it seems likely that conjoining NeoAg peptide will generally achieve superior results, but universal helper epitopes may be necessary when only $CD8^+$ T cell-reactive neoantigens have been identified following *in silico* prediction. Neoantigen vaccinations are frequently combined with ICB to empower the primed response in both mouse studies[108–110] and clinical trials[111–113].

ACT aims to circumvent the rarity of tumor-specific host T cells and the immunosuppressive environment of the TME by transferring therapeutically potent T cells in mass quantities. There are two ways of obtaining these cells: Either isolating a polyclonal population of tumor-infiltrating lymphocytes (TIL) for *in vitro* expansion and activation or using gene therapy to engineer circulating T cells so they target specific antigens[114,115].

TIL are presumed to have a high concentration of tumor-specific T cells that were able to invade the TME but have been exhausted, suppressed, or primed in such a way that they exhibit only a modicum of their potential function[116]. Many groups have tried leveraging these cells by isolating them from patients, expanding and reinvigorating them with cytokine regiments including IL-2[117] and IL-12[118], then reintroducing them to the patient[119–123]. This polyclonal population may be harnessed and prepared more quickly than personalized antigen-specific treatments while being less susceptible to downregulation of a single targeted antigen and thus immune escape. However, the mixed success of this method has necessitated more specific therapies that don't rely on finding potentially rare tumor-specific T cells able to be reinvigorated[124].

Specificity comes from inducing TCRs that recognize either neoantigens[125,126] or chimeric antigen receptors (CAR) targeting tumor-associated antigens like CD19 uniformly expressed in B-cell malignancies[127–130]. Human PBMC or mouse splenocytes are harvested and the desired cell type is isolated. The cells are activated, transduced with the desired TCR, and differentiated using cytokines like IL-2 or IL-7 and IL-15 prior to injection into the patient[131]. Initial studies primarily focused on transferring cytotoxic $CD8^+$ T cells[132], but the importance of $CD4^+$ T cells during these treatments necessitated transferring both populations in future clinical trials[133–136]. Studies suggest the phenotype of these cells is very important and that cells induced to adopt less differentiated phenotypes are therapeutically superior to those adopting a central memory phenotype[137–139].

Though cells leveraged this way only target one specific antigen, there's ample evidence suggesting that ACT can be sufficient to induce epitope spreading[140–142], likely

because the transferred cells kill tumor cells and cause the release of other neoantigens picked up by macrophages and dendritic cells.

Given the range of potent effector pathways available to natural NeoAg-specific $CD4^+$ T cells for the control of incipient cancers as well as the ability of immunotherapies to leverage these cells, the progressive outgrowth of primary and metastatic tumors suggests that these cells either do not properly expand or are actively suppressed under physiologic conditions. The former could involve a failure at any number of levels in the generation of $CD4^+$ T cells including antigen presentation, engagement of the proper TCR repertoire, colocalization of pAPCs and $CD4^+$ T cells, clonal expansion, or effector development. The latter could involve various immunosuppressive mechanisms, including the action of tumor specific Tregs or deviation into functional subsets that are unable to mediate tumor control. Distinguishing among these possibilities has been difficult as the developmental course of NeoAg-specific $CD4^+$ T cells responding to progressive tumor growth *in vivo* is largely unknown in terms of phenotype, magnitude, and TCR repertoire.

We have addressed these questions in an aggressive low tumor mutational burden (TMB) preclinical tumor model SCC VII, which closely resembles human head and neck squamous cell carcinomas in its high incidence of metastasis, poor immunogenicity, and resistance to common immunotherapeutic interventions. Previous work within our lab demonstrated that SCC VII generates $CD4^+$ and $CD8^+$ T cells specific for a set of 5 NeoAg following whole cell vaccination[143]. Of these five peptides, four are recognized strictly by $CD4^+$ T cells while a clathrin mutation named Mut_48 ($CLTC_{H129>Q}$) is recognized by both $CD4^+$ T cells and $CD8^+$ T cells. Given the importance in leveraging both $CD4^+$ T cells and

$CD8^+$ T cells for optimal immunotherapeutic results, it is unsurprising that this previous work in the lab also showed that immunotherapeutic vaccination with Mut_48, but not neoantigens solely recognized by $CD4^+$ T cells, significantly reduced tumor burden in the less aggressive GFP/Luciferase-transfected SCC VII line. The parental SCC VII line offered the opportunity to study $CD4^+$ T cells specific for a therapeutically relevant neoantigen in a poorly immunogenic and aggressive tumor model. I set out to understand the roles endogenous NeoAg-specific $CD4^+$ T cells play within the context of growing tumors and how successful immunotherapeutic vaccination perturbs these cells to achieve this.

Using $CLTC_{H129>Q}/I\text{-}A^k$ tetramers to isolate and characterize $Cltc_{H129>Q}$-specific $CD4^+$ T cells during progressive growth of SCC VII tumors, our data reveal that the NeoAg-specific $CD4^+$ T cell response is functionally and phenotypically diverse, containing Treg, Tfh-like, and Th1 cells expressing TCRs of varying affinity within its repertoire. This response is multifaceted even during the initial expansion shortly after tumor inoculation, showcasing for the first time the early rise of NeoAg-specific Tregs. The response is also dynamic, as the relative ratios of these subsets changes over time and in response to combined immunotherapy with peptide vaccination and αPD-1. This treatment significantly increases the frequency of $CD4^+$ T cells able to recognize the peptide used for vaccination while simultaneously reducing the frequency of NeoAg-specific Tregs in both the tdLN and within the tumor itself.

We used single cell transcriptomics to confirm these findings and to investigate the TCR repertoire of the response. We identified at least 11 different TCR α/ß pairs within the tdLN of tumor-bearing animals generated by an endogenous response that bound the

Cltc$_{H129>Q}$/I-A^{k} tetramer. This polyclonal response exhibited a range of phenotypic subsets and most individual TCRs were expressed by multiple phenotypic subsets of cells. TCR retroviral transduction allowed for the expression and subsequent characterization of confirmed NeoAg-specific TCRs, which revealed a 17.75 fold range in TCR affinity and that were was no correlation between TCR affinity and the phenotypic fate of cells expressed each TCR in the endogenous response. Finally, our data show that ACT with Tscm cells transduced to express NeoAg-specific TCR are similarly able to mediate immunotherapy regardless of TCR affinity or the phenotypic subsets of cells on which the TCR was found as even a very low affinity TCR found solely on a single Treg was able to cause clearance of established tumors following chemotherapy. This provides an unprecedented insight into the ontogeny of the natural spontaneous NeoAg-specific CD4^{+} T cells responding to progressive tumor growth in the absence of other manipulation and how therapeutic NeoAg vaccination influences this development.

CHAPTER 1: Defining the role of NeoAg-specific CD4+ T cells in the outgrowth of an aggressive MHC-II-negative squamous cell carcinoma.

Identification of a therapeutically relevant CD4$^+$ T cell-reactive Neoantigen in SCC VII

Vaccination with a 20mer neoantigen peptide induces an antigen-specific response in splenocytes that can be recalled during an ELISpot for three of the five mutations, including Mut_48 (Figure 2a). Peptide vaccination with Mut_48 induces both a CD8$^+$ and CD4$^+$ T cell response even when administered as free peptide (Figure 2b) and the use of a $CLTC_{H129>Q}$-containing 10mer minimal epitope (48.10) is still capable of engaging both CD4$^+$ and CD8$^+$ T cells (Figure 2c). Though it is rare for the epitope a CD4$^+$ T cell recognizes to be so short, it isn't unheard of[144] and unfortunately precludes neoantigen vaccination of solely CD8$^+$ T cells. Taken together, these data lend credence to the idea that immunotherapeutic vaccination with Mut_48 reduces tumor burden in a way vaccination with other neoantigens don't because only Mut_48 activates both neoantigen-specific CD4$^+$ and CD8$^+$ T cells. This requires both immune checkpoint blockade in the form of αPD-1 and neoantigen vaccination comprised of polyI:C as an adjuvant alongside the neoantigen peptide, as using only one arm of this dual therapy did not significantly reduce tumor burden (Figure 2d).

Using antibodies to either block CD40:CD40L interactions or deplete CD4$^+$ T cells after therapeutic vaccination begins partially but doesn't fully ablate the efficacy of treatment (Figure 2e). This confirms that help signals provided by CD4$^+$ T cells

recognizing their cognate antigen on pAPCs expressing CD40 are required throughout the entirety of tumor growth to achieve the full effect of therapy and are not solely needed to license dendritic cells for the initial priming of a $CD8^+$ T cell response. While the fact that $CD4^+$ T cell depletion causes the same effect on tumor burden seems to suggest that providing help signals through CD40:CD40L interactions is the sole role of $CD4^+$ T cells in this model, $CD4^+$ T cell depletion also gets rid of immune suppressive Tregs that should be actively inhibiting the rest of the immune response. This suggests that there is an additional role for $CD4^+$ T cells in promoting anti-tumor immunity and that their loss offsets the enhanced effect other immune cells have without the constraint of Tregs. These $CD4^+$ T cells are needed throughout tumor development and their sole role is not to provide help signals during the initial priming of $CD8^+$ T cells. Importantly, though the endogenous response is insufficient to protect the animal from tumor even when aided by checkpoint blockade, the immune system has neoantigen-specific T cells that can be induced to significantly reduce tumor burden. This prompted study of $CLTC^{H129>Q}$-specific $CD4^+$ T cells.

Natural NeoAg-specific $CD4^+$ T cells expand over the course of tumor growth but can be further expanded by therapeutic vaccination

To study the development of the endogenous $CLTC_{H129>Q}$-specific $CD4^+$ T cell response to a developing tumor, tdLN lymphocytes were isolated at 3-day intervals beginning 6 days after tumor inoculation. Staining with $CLTC_{H129>Q}$/I-A^k tetramer revealed

a distinct population of NeoAg-specific T cells (Figure 2f) first seen nine days after tumor inoculation which expanded throughout tumor growth without intervention, ultimately comprising approximately 0.1% of total $CD4^+$ T cells in the tdLN (Figure 2g, closed symbols). $CLTC_{H129>Q}$/I-A^k-specific responses were also monitored at 12- and 18-days post tumor inoculation in animals undergoing therapeutic vaccination, which approximately doubled the response's magnitude at the later time point (Figure 2g, open symbols). This confirmed that immunotherapeutic vaccination induces expansion of cells specific for the neoantigen used but left questions about the phenotypes these cells express and whether immunotherapeutic intervention alters the relative ratios of certain subsets or whether it reduces tumor burden solely by inducing an expansion of NeoAg-specific $CD4^+$ T cells.

Acknowledgements

The bulk of this chapter is sourced from a manuscript entitled "The spontaneous neoantigen-specific CD4+ T cell response to a growing tumor is functionally and phenotypically diverse." currently being submitted for review. As such, I'd like to thank my co-authors Spencer E. Brightman, Karla Soria Zavala, Manuel Azaid Ordaz-Arias, Navid Djassemi, Rukman R. Thota, Martin S. Naradikian, Hannah Dose, Suzie Alarcon, Vijayanand Pandurangan, Bjoern Peters, Arron M Miller, Ezra E. W. Cohen, and Stephen P. Schoenberger.

CHAPTER 2: A complete longitudinal phenotypic characterization of the natural NeoAg-specific CD4+ T cell response throughout progressive tumor growth and in response to therapeutic vaccination.

Characterization of draining lymph node-resident total and NeoAg-specific CD4$^+$ T cells

Total and tetramer-positive CD4$^+$ T cells were further analyzed by flow cytometry for the functional subset-defining markers CXCR3 (Th1), FoxP3 (Treg), and CXCR5$^+$/PD-1^{hi} (Tfh-like). The gating strategy used to identify these cells is shown in figure 3a for total (top row) and tetramer-positive (bottom row) CD4$^+$ T cells. The relative ratio of functional subsets within the total CD4$^+$ T cell compartment in the tdLN showed little change over time (Figure 3b), while the CLTC$_{H129>Q}$/I-A^k-specific CD4$^+$ T cell response was found to be comparatively diverse, involving all three functional subsets at higher frequencies than observed among total CD4$^+$ T cells (Figure 3c, closed symbols). The relative frequencies of each subset varied over time and was further affected by therapeutic vaccination (Figure 3c, open symbols). NeoAg-specific Th1 cells were detected 9 days post tumor inoculation and their frequency within the tdLN rapidly declined from approximately 25% to approximately 3% of NeoAg-specific CD4$^+$ cells over time regardless of therapeutic intervention. Within the same time frame, the frequency of NeoAg-specific Tregs steadily increased from 18% to 24% within the tdLN. Notably, this was reversed in animals undergoing therapeutic vaccination, which exhibited a significantly reduced frequency of NeoAg-specific Tregs of approximately 5% by day 18. CXCR5$^+$ PD-1$^+$ Tfh-like cells that

made up a minor fraction of total $CD4^+$ T cells were a significant component of the $CLTC_{H129>Q}$-specific response, and these also subsequently deceased during progressive tumor growth. Taken together, these results demonstrate that the $CLTC_{H129>Q}/I\text{-}A^k$ tetramer allows the primary NeoAg-$CD4^+$ T cell response to be visualized and phenotyped within the tdLN during progressive outgrowth of SCC VII tumors. The response is both diverse and dynamic, comprising a range of functional subsets that appear with distinct kinetics and relative magnitudes.

Characterization of tumor-resident total and NeoAg-specific $CD4^+$ T cells

To characterize the total and NeoAg-specific $CD4^+$ T cells within the TME, TIL were isolated 12- and 18-days after tumor inoculation from untreated animals and those undergoing therapeutic vaccination. In the absence of vaccine therapy, the frequency of total $CD4^+$ T cells infiltrating the tumor decreased over time (Figure 4a). $CLTC_{H129>Q}/I\text{-}A^k$-specific cells were present within the tumor at both time points and made up a larger percentage of tumor-infiltrating $CD4^+$ T cells at day 18 (Figure 4b). Most $CD4^+$ T cells in the tumor had an activated phenotype, with more than 60% expressing PD-1 (Figure 4c). Tregs were the dominant phenotype amongst these cells at both time points. Tregs were also the largest subset among tumor-infiltrating $CLTC_{H129>Q}/I\text{-}A^k$-specific cells in untreated animals, but therapeutic vaccination significantly reduced their frequency 18 days post tumor inoculation from 61% in untreated animals to 18% in vaccinated animals (Figure 4d), which parallels the effect of therapeutic vaccination on $CLTC_{H129>Q}/I\text{-}A^k$-specific

Tregs in the tdLN (Figure 3c). Though therapeutic vaccination did not effect the frequency of PD-1 expression on $CLTC_{H129>Q}$-specific Tregs, it significantly reduced the frequency of PD-1 expression amongst total tumor-infiltrating Tregs from 88% to 68%. These data reveal key similarities and differences between the NeoAg-specific $CD4^+$ T cell response within the tumor and draining lymph node, with the early appearance and increasing presence of $CLTC_{H129>Q}$-specific Tregs in both locations offering possible clues into how an initial Th1 response is followed by a potent population of NeoAg-specific regulatory cells.

Acknowledgements

This chapter is sourced from a manuscript entitled “The spontaneous neoantigen-specific CD4+ T cell response to a growing tumor is functionally and phenotypically diverse.” currently being submitted for review. As such, I’d like to thank my co-authors Spencer E. Brightman, Karla Soria Zavala, Manuel Azaid Ordaz-Arias, Navid Djassemi, Rukman R. Thota, Martin S. Naradikian, Hannah Dose, Suzie Alarcon, Vijayanand Pandurangan, Bjoern Peters, Arron M Miller, Ezra E. W. Cohen, and Stephen P. Schoenberger.

CHAPTER 3: Single-cell transcriptional profiling of NeoAg-specific CD4+ T cells during progressive tumor growth

Single-cell genomic analysis of the natural $CLTC_{H129>Q}$-specific $CD4^+$ T cell response

We sought to better understand key features of the spontaneous $CLTC_{H129>Q}$/I-A^k-specific response that may explain its dynamic nature by comparing the transcriptional profiles and TCR repertoire of single cells. Figure 5a diagrams the approach used to obtain single-cell RNA and TCR data through the 10X platform. Global gene expression profiling of sorted $CLTC_{H129>Q}$/I-A^k tetramer-positive versus tetramer-negative cells showed that these populations are remarkably distinct, with the majority of tetramer-negative cells expressing a naïve phenotype (Figure 5b and Supplemental Figure 1). Tetramer-positive cells, in contrast, were antigen-experienced and had differentiated into specific functional subsets (Figure 5c) including stem-like cells with high levels of TCF1 and few markers of differentiation, Th1 cells that express higher levels of Ifng and TNF, regulatory cells with high levels of IL-10, Lag-3, and IL-2ra, and Tfh-like cells expressing high levels of IL-6, CXCR5, and Bcl6 (Figure 5d). Vβ family analysis indicated a higher degree of clonal expansion in tetramer-positive than in tetramer-negative cells (Figure 45). These data demonstrate a remarkably high degree of phenotypic heterogeneity present at the single cell level within the endogenous primary NeoAg-specific $CD4^+$ T cell response to a developing tumor.

Developmental plasticity within the Cltc$_{H129>Q}$-specific TCR repertoire

We next examined the phenotype of CD4$^+$ T cells expressing distinct NeoAg-specific TCRs. Individual α/β TCR clonotypes isolated from CLTC$_{H129>Q}$/I-A^k-binding cells (Table 1) were expressed in primary C3H CD4$^+$ T cells by retroviral transduction using a variant of the pMSGV1 vector diagramed in figure 6a encoding TCR genes upstream of CD90.1, which was used as a transduction reporter. This enabled measurement of the relative transduction efficiency and surface TCR expression using Vβ and CD90.1 as surrogates (Figure 6b). TCR clonotypes that successfully bound CLTC$_{H129>Q}$/I-A^k tetramer (Table 2) were then mapped back to the differential gene analysis for quantification of their clustering (Figure 6c and 6d). This analysis revealed that nearly every TCR was found in multiple clusters, with no clear preference for any individual TCR to limit the range of fates it was able to adopt. These findings demonstrate that, rather than being constrained to a specific functional subset, different developmental fates are available to cells expressing the same clonal TCR.

Acknowledgements

This chapter is sourced from a manuscript entitled “The spontaneous neoantigen-specific CD4+ T cell response to a growing tumor is functionally and phenotypically diverse.” currently being submitted for review. As such, I’d like to thank my co-authors Spencer E. Brightman, Karla Soria Zavala, Manuel Azaid Ordaz-Arias, Navid Djassemi, Rukman R. Thota, Martin S. Naradikian, Hannah Dose, Suzie Alarcon, Vijayanand

Pandurangan, Bjoern Peters, Arron M Miller, Ezra E. W. Cohen, and Stephen P. Schoenberger.

CHAPTER 4: Functional characterization and therapeutic potential of high- and low-affinity TCRs isolated from natural NeoAg-specific CD4+ T cells.

Functional characterization of the Cltc$_{H129>Q}$--specific TCR repertoire

We next investigated whether the affinity of a given TCR influences the developmental fate of the T cells expressing it. This was done by titrating the concentration of tetramer used during staining (Figure 7a) and normalizing differences in retroviral transduction efficiency between TCRs using a ratio of the mean fluorescent intensity of CLTC$_{H129>Q}$-tetramer and the CD90.1 reporter (Figure 7b). The 11 distinct validated NeoAg-specific TCRs have a wide range of affinities, including a 17.75 fold range at the standard working tetramer concentration of 2µg/mL used in previous experiments (Figure 7c). We then mapped the affinity of each TCR back to the UMAP used to determine phenotypic clustering in Figure 5c (Figure 7d). This revealed that each functional subset was adopted by TCRs with a wide range of affinities without any correlation between TCR affinity and the phenotypes adopted. (Figure 7e).

To further demonstrate that TCR affinity does not determine phenotypic fate or function, we asked whether TCRs isolated from Tregs could nonetheless mediate therapeutic efficacy when used for ACT. To examine this, primary CD4^{+} T cells were transduced with TCR1, a high-affinity TCR which we have previously shown can mediate tumor rejection in the context of ACT, or with either TCR16 or TCR18, both of which were isolated from a single Treg. Following TCR engineering, the transduced cells were

cultured with IL-7 and IL-15 to induce a Tscm phenotype prior to adoptive transfer into cyclophosphamide-conditioned C3H mice bearing established SCC VII tumors inoculated 8 days prior. Despite a 12.67-fold range of affinities between the distinct TCRs and a 3.95-fold difference in transduction efficiency (Supplementary Figure 2), all three TCRs were able to successfully produce tumor clearance in 3 out of 4 animals while transfer of mock transduced polyclonal cells had no discernable effect (Figure 7f). Additionally, $CD90.1^+$ cells were found at comparable levels in the tdLN 19 days after injection without any apparent correlation between the TCR they expressed and either the frequency of $CD90.1^+$ cells or the residual tumor burden (Figure 7g).

Acknowledgements

This chapter is sourced from a manuscript entitled “The spontaneous neoantigen-specific CD4+ T cell response to a growing tumor is functionally and phenotypically diverse.” currently being submitted for review. As such, I’d like to thank my co-authors Spencer E. Brightman, Karla Soria Zavala, Manuel Azaid Ordaz-Arias, Navid Djassemi, Rukman R. Thota, Martin S. Naradikian, Hannah Dose, Suzie Alarcon, Vijayanand Pandurangan, Bjoern Peters, Arron M Miller, Ezra E. W. Cohen, and Stephen P. Schoenberger.

DISCUSSION

Tumor-specific $CD4^+$ T cell responses have traditionally been studied using model antigens and in the 'post-hoc' setting following their generation by targeted vaccination, immune checkpoint blockade, or at late stages of tumor outgrowth. Although such studies have been instrumental in revealing the various effector and regulatory roles of $CD4^+$ T cells in tumor immunity, none have allowed insights into the natural ontogeny of tumor-specific $CD4^+$ T cells in unmanipulated conditions. The availability of a $CLTC_{H129>Q}$/I-A^k tetramer has enabled the characterization of the natural $CD4^+$ T cell response to a validated NeoAg for the first time. SCC VII is an aggressive and poorly immunogenic tumor and natural $CLTC_{H129>Q}$-specific cells are unable to mediate a productive anti-tumor response. However, the effect CD4 depletion and CD40:CD40L blockade have on reducing the effect of therapeutic intervention show that the tumor-specific cells maintain an important role throughout tumor growth and that these cells can be induced to mediate a significant reduction in tumor volume following targeted immunotherapeutic vaccination. We investigated progressively growing endogenous tumors and tumors growing in mice being treated with a combination of neoantigen vaccination and immune checkpoint blockade to study the TCR repertoire, phenotypic fates, and relative functional avidity of different subsets of NeoAg-specific $CD4^+$ T cells.

Flow cytometry analysis reveal that the endogenous $CD4^+$ T cell response to a cross-presented MHC-II-restricted neoantigen is both diverse, involving differentiation into several distinct functional subsets, and dynamic, with the relative frequencies of regulatory and different effector subsets changing over time with progressive tumor

growth and in response to therapeutic vaccination. These findings were recapitulated and extended using single-cell transcriptomics to verify the gene expression programs that characterize the diverse $CLTC_{H129>Q}$/I-Ak-specific $CD4^+$ T cell response, which echoed what was found in our multimodal phenotypic analysis by showing that the initial response within the tdLN is comprised of Th1, Tfh-like, and Treg cells. We also demonstrated that the endogenous neoantigen-specific $CD4^+$ T cell response is polyclonal by analyzing the set of TCRs identified among $CLTC_{H129>Q}$/$I\text{-}A^k$ tetramer-positive cells during single-cell transcriptomics. We then used the NeoAg-specific TCRs identified using single-cell transcriptomics for TCR engineering to probe the TCR repertoire, which revealed that there was no correlation between a TCR's affinity the phenotypes adopted by cells expressing the TCR. Lastly, we showed that all tested TCRs were equally able to mediate therapy when primary $CD4^+$ T cells were genetically engineered to express a NeoAg-specific TCR prior to conditioning into a Tscm-like Th1 cell and used in adoptive cell therapy.

The frequency of NeoAg-specific Th1 cells significantly decreases in the tdLN throughout tumor growth. Given the much higher frequency of total Th1 cells within the both the tumor-draining lymph node and tumor microenvironment 18 days post tumor implantation compared to 12 days post tumor implantation as well as the high frequency of NeoAg-specific Th1s within the tumor at this later time point, it seems likely that Th1 cells preferentially traffic to the tumor microenvironment. The full role Th1 cells have within the TME was beyond the scope of this study but given that therapeutic vaccination increases the frequency of total but not NeoAg-specific Th1 cells in both locations, it's unclear if the elevated levels of Th1 cells seen within the TME at the later timepoint is a

result of elevated NeoAg levels caused by dying tumor cells or the result of αPD-1 or polyI:C altering the trafficking, expansion, and/or differentiation of Th1 cells.

Therapeutic vaccination with the mutated $CLTC_{H129>Q}$ peptide, polyI:C, and αPD-1 significantly reduces the frequency and the total number of NeoAg-specific Tregs in both the tdLN and TME 18 days after tumor inoculation (Figure 3b and 4d). Given the early rise of NeoAg-specific Tregs as soon as 9 days post tumor implantation and that therapeutic vaccination did not reduce the frequency of total Tregs, the observed reduction in NeoAg-specific Tregs seems to be specific to the antigen included in the vaccine. As this is the sharpest change in NeoAg-specific $CD4^+$ T cells achieved by therapeutic vaccination, it calls to question if this is the main mechanism through which the combined therapies leverage $CD4^+$ T cells to reduce tumor burden. If so, the fact that total Treg levels are unaffected suggests that NeoAg-specific Tregs are more important for suppressing the immune response than the plethora of other Tregs within the tumor and tumor-draining lymph node, though no mechanism for this is known. Another mouse model with known neoantigen-specific tetramers that allows for Treg-specific deletion or tracking, such as in a B6 mouse, would be invaluable in answering these questions.

Our data clearly show that the $CLTC_{H129>Q}$/I-A^k-specific $CD4^+$ T cell response is oligoclonal and comprised of TCRs exhibiting a range of affinities. However, most TCRs were expressed by a range of phenotypes and TCR affinity did not appear to correlate with the phenotypic fates of each clone and (Figure 7d). We adoptively transferred primary $CD4^+$ T cells retrovirally-transduced to express a NeoAg-specific TCR found during the endogenous response into chemotherapy-treated tumor-bearing animals. All tested NeoAg-specific TCRs, including the lowest affinity TCR identified as being

expressed solely by a single Treg, were capable of mediating tumor clearance to a comparable extent and were found within the tumor-draining lymph nodes at similar frequencies independent of the functional subset from which the TCR was identified, TCR affinity, or transduction efficiency. Given that Tregs can be found amongst NeoAg-specific cells at the earliest time points the response can be identified and that the most dramatic effect that successful immunotherapeutic vaccination has was the decrease in NeoAg-specific Treg frequency in both the tdLN and TME, these findings raise the interesting possibility that a therapy capable of converting early-rising NeoAg-specific Tregs into anti-tumor phenotypes or favoring the expansion of anti-tumor NeoAg-specific $CD4^+$ T cells would be extremely potent.

There is mixed evidence suggesting that the affinity of $CD8^+$ T cell TCRs for their cognate antigen influences their fate or therapeutic potential[145,146]. The critical role for cytokines in determining the fate of $CD4^+$ T cells lends credence to the idea that TCR affinity plays a limited or negligible role compared to the surrounding environment during their initial priming and differentiation. Given the diversity of the initial NeoAg-specific $CD4^+$ T cell repertoire as soon as the response is able to be detected, it's unclear if the changes to the relative ratios of phenotypic subsets throughout tumor growth are a result of changing conditions for initial priming of newly activated clones caused by the growing tumor or if the changes are a result of the environments, APC types available, and accessory signals the NeoAg-specific $CD4^+$ T cells are exposed to after their priming inducing either preferential division in a limited subset of phenotypes or plasticity in the ongoing response.

These findings offer the first look into the form and functionality of a developing natural NeoAg-specific $CD4^+$ T cell response. Our data reveals the range of functional subsets that the response can comprise and demonstrates how combined neoantigen therapy and αPD-1 immune checkpoint blockade may alter these and reduce tumor burden. Additionally, our study shows the diversity of the response to a single neoantigen can generate clonal T cells which can adopt a range of developmental fates that are independent of their TCR avidity. These insights will aid in understanding the diversity and functionality of antitumor $CD4^+$ T cell responses and should allow the development of strategies through which these can be therapeutically manipulated to favor tumor control.

ACKNOWLEDGEMENTS

Chapters 1, 2, and 3 are largely based upon a paper being submitted out for peer review at Nature Cancer. The dissertation author was the primary investigator and author of this material.

METHODS

Animals

Male and female C3H/HeJ mice (The Jackson Laboratory, Bay Harbor, ME) were used in these experiments. Animals used were 7-12 weeks of age and maintained/bred in the La Jolla Institute for Immunology vivarium with pathogen-free conditions in accordance with guidelines of the Association for Assessment and Accreditation of the Laboratory Animal Care International.

Cell Culture

Squamous cell carcinoma VII San Francisco (SCC VII) is a tumor line which spontaneously arose in the abdominal wall of a C3H mouse at the laboratory of Herman Suit (Harvard University, Cambridge, MA) and was adapted for *in vitro* growth by Karen k. Fu and Kitty N. Lam (University of California, San Francisco, CA). SCC VII was maintained for a maximum of 3 passages *in vitro* in RMPI 1640 media with 12.5% fetal bovine serum (FBS) and 100 units/mL each of penicillin/streptomycin (Gibco). Vials of P0 SCC VII cells were obtained by injecting female C3H/HeJ mice subcutaneously (S.C.) with $5x10^5$ P2 cells in 1x DPBS and harvesting tumors 14 days after inoculation. Tumor tissue was dissociated with the mouse Tumor Dissociation Kit (Miltenyi Biotec, Aubrun, CA), passed through a 70µm cell strainer (Fisher Scientific, Pittsburgh, PA), and resuspended in media for *in vitro* passage. The reporter SCC VII line expressing luciferase and copepod-derived GFP cells were originally transduced with the

BVLIV713VA-1 HIV lentiviral vector (System Biosciences, Palo Alto, CA), exposed to 10µg/mL puromycin selection, then further purified using FACS-sorting to isolate GFP^+ cells.

Injections & in vivo treatments

SCC VII tumors were generated by injecting $5x10^5$ cells in 100µL 1x DPBS S.C. of either the parental or reporter line. Peptide vaccinations were carried out 6 and 15 days post tumor inoculation in the parental SCC VII line and 10 and 19 days post tumor inoculation in the SCC VII reporter line by injecting 100µg peptide and 50µg Poly(I:C) combined in 100µL of 1x DPBS S.C. directly anterior to the growing tumor. Immune checkpoint blockade was carried out by intraperitoneal (I.P.) injection of 200µg of αPD-1 (Clone RMP1-14, Bio X Cell) compared to polyclonal rat IgG2b κ (Bio X cell) as an isotype control every 3 days starting concurrently with peptide vaccination. CD4 depletion was achieved by I.P. injection of 400ug αCD4 (Clone GK1.5, in house) compared to polyclonal rat IgG2b κ (Bio X cell) as an isotype control 9 days after tumor inoculation. CD40/CD40L was blocked by I.P. injection of 200ug αCD40L (MR1, Bio X Cell) compared to polyclonal Aremnian hamster IgG (Bio X Cell) isotype control every 2 days beginning 9 days after tumor inoculation. Tumor volume was calculated using the equation $V = L/2*W^2$ where L represents the longest length of the tumor and W represents the width perpendicular to the longest length. Prior to the first round of treatments, tumors were measured and groups were normalized.

Preparation of single cell suspensions

Lymph nodes were surgically removed and dissociated manually via passage through a 70µm strainer. Tumors were surgically removed and cut into small (<2mm) pieces. The fragments were enzymatically dissociated in 20 µg/mL Liberase (Roche) and 20 µg/mL DNase I (Roche) at 37 degrees for 45 minutes. They were shaken at the 15 and 30 minute marks. Afterwards, they were passed through a 70 µm strainer.

Flow cytometry

Prior to staining, Fc receptors were blocked with αCD16/32 (Clone 2.4G2, BD Biosciences) for 15 minutes at 4C. Tetramer staining was carried out using PE- or APC-conjugated I-A^k(VALVTDNAVYQWSME) or CLIP tetramer PVSKMRMATPLLMQA. They were incubated at the indicated concentration in FACS buffer (PBS + 1% bovine serum albumin + 0.1% sodium azide) at 37C for 1 hour. Surface antigens were stained with the indicated antibodies for 20 minutes on ice. Dead cells were excluded using either DAPI immediately prior to reading or Fixable Viability Dye eFlour 780 (ThermoFisher) prior to surface staining. Transcription factor staining was carried out using the eBioscience Foxp3 / Transcription Factor Staining Buffer Set (eBioscience) according to manufacturer guidelines. All flow cytometry was performed on a BD FACS Celesta or BD LSR-II and analyzed using FlowJo.

Single cell genomics

Single-cell (sc)RNA-seq reads were demultiplexed into individual libraries (n=12). Demultiplexing was executed using Illumina's bcl2fast software (v2.19.0.316). The individual libraries underwent processing with 10x Genomic's Cell Ranger software (3.1.0). The module count was employed to align and map the reads to the mm10 reference mouse genome (v3.0.0). Unique molecular identifier (UMI) counts for each cell barcode associated with each gene. Gene expression data from the individual libraries were aggregated into a single dataset that included both tetramer-positive and tetramer-negative cells.

The Seurat toolkit (v3.1.5) was employed to conduct the analysis of the aggregated scRNA-seq dataset. Genes expressed by less than 0.1% of the cells in the dataset were excluded from the analysis. T-cell receptor TCR (annotations) were performed as a distinct step (described below). To reduce the occurrence of potential doublets and transcriptomes of low quality, the barcodes that did not meet the following criteria were filtered out: UMI counts between 500 and 15,000, gene counts between 300 and 4,500, and a mitochondrial UMI percentage not exceeding 10%.

The data of the aggregated dataset was normalized using the NormalizeData function in Seurat (default parameters). The most variable genes were identified as those with a mean UMI capture greater than 0.01, contributing to 25% and 10% of the total standardized variance in the aggregate dataset. This selection process was carried out by applying the variance-stabilizing transformation method through the function FindVriableFeatures (default parameters). Data scaling was performed using the ScaleData function, with custom variables regressed out using the 'vars.to.regress' parameter. Cell clusters were determined within the aggregated dataset using the

FindNeighbors and FindClusters functions, primarily with default parameters, except for the number of principal components (PCs; PCs=20) and the 'resolution' parameter (res). The RunUMAP function was applied with the top 40 PCs, 15 neighboring points for local approximations of the manifold structure, and a minimum distance of 0.1 (specified as arguments dims, n.neighbors, and min.dist, respectively) to compute manifold approximation and projection (UMAP) embeddings. Various plot types were generated using custom scripts, primarily based on ggplot2, an open-source data visualization package for the R statistical programming language, and are available from the GitHub repository (Github repo).

TCR cloning and expression

TCR amino acid sequences were constructed from single cell genomics data. DNA sequences were generated using NovoPro ExpOptimzer. The sequences were synthesized and cloned into MSGV1 retroviral expression backbones using BioXP (Codex DNA, San Diego CA). TCR alpha and beta chains were separated from each other and a flanking CD90.1 sequence with a P2A ribosomal skipping element. TCR retroviral supernatants were harvested 48 and 72 hours after cotransfection of Platinum-Eco cells with the TCR-containing retroviral vectors and pcL-Eco. Supernatants were stored at -80C. For transfection of mouse primary cells, spleens from naïve C3H/HeJ mice were manually dissociated. Cell suspensions were passed through a 70 µm filter. $CD4^+$ T cells were isolated by magnetic negative selection (StemCell) then stimulated for 24 hours with anti-CD3/CD28 Dynabeads (Gibco) in T cell media (RPMI 1640 + 10% FBS + 50µM beta-mercaptoethanol, 1x, penicillin/streptomycin and HEPES). Non-tissue

Culture-Treated 24 well plates (Falcon). were coated with 10µg/mL retronectin overnight at 4C. They were washed with 2% BSA in HBSS for 30 minutes at room temperature, then retroviral supernatants were spun down at 2000g for 2 hours at 32C. After discarding the supernatant, 1 million activated mouse primary cells were spun down in each well at 500g for 10 minutes with break and acceleration of 1.

Statistics

Statistical analyses were performed with Prism 8 (Graphpad Software). For ICS comparisons, an unpaired T test was used. **Repeat this for everything.**

Figure 1: The multi-faceted roles of neoantigen-specific CD4$^+$ T cells in mediating anti-tumor immunity.

Following antigen recognition in the tdLN, CD4$^+$ cells license dendritic cells to improve their ability to activate CD8+ T cells. They also prime B cells to promote tumor-specific antibodies. Activated CD4+ T cells may also migrate to the tumor microenvironment. There, they can potentially recognize MHC-II-positive tumors directly or recognize their antigen on macrophages and other pAPCs. They're able to induce a tumorcidal phenotype in macrophages, inhibit vasculature development, improve CD8+ T cell and NK cell cytot oxic functions, and induce senescence in cancer cells through cytokine secretion.

Created with BioRender.com

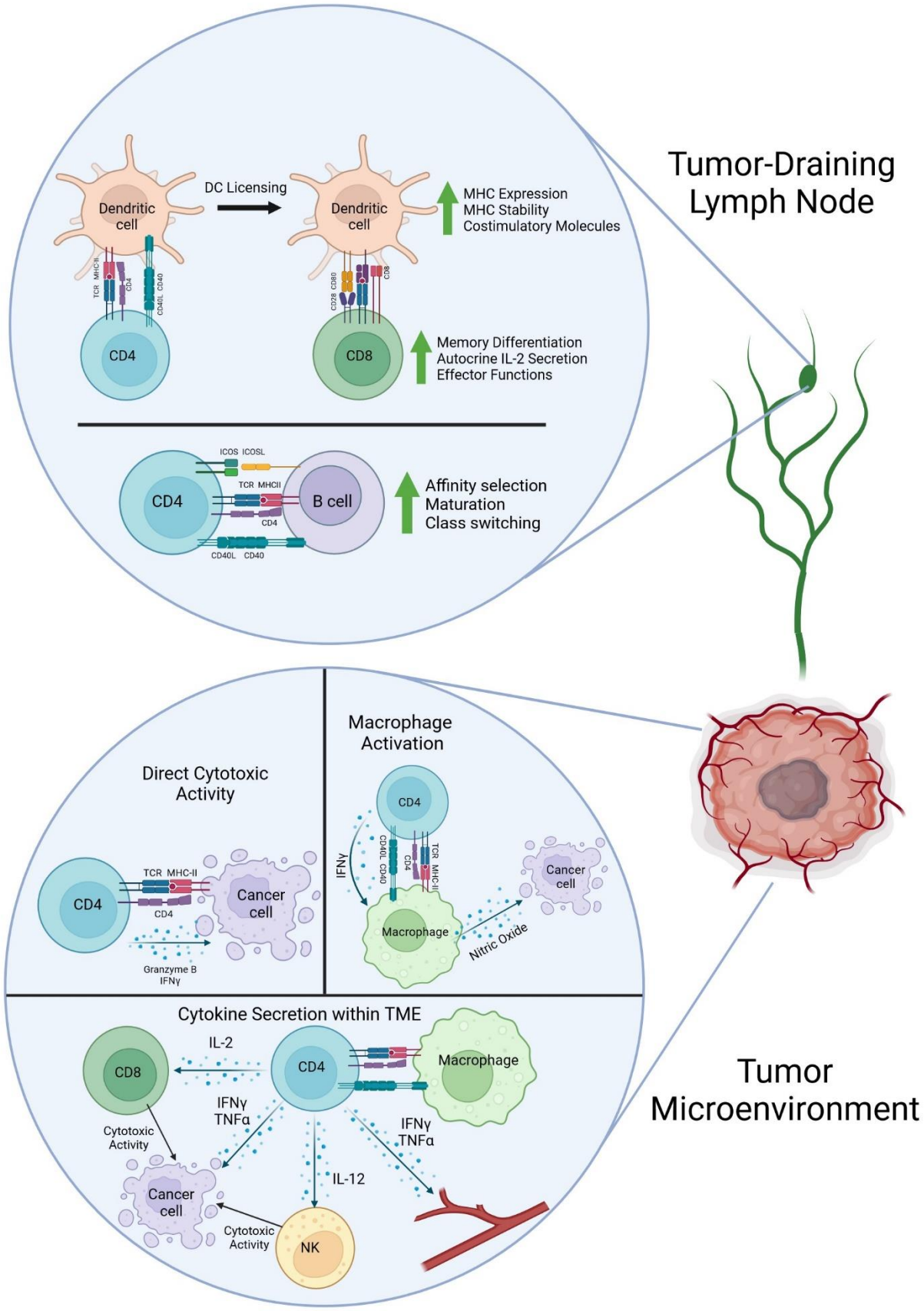

Tumor-Draining Lymph Node
Dendritic cell
DC Licensing
Dendritic cell
MHC Expression
MHC Stability
Costimulatory Molecules
TCR MHC-II
CD4
CD40L CD40
CD4
CD28 CD80
CD8
CD8
Memory Differentiation
Autocrine IL-2 Secretion
Effector Functions
ICOS ICOSL
TCR MHCII
CD4
CD4
B cell
CD40L CD40
Affinity selection
Maturation
Class switching
Direct Cytotoxic Activity
CD4
TCR MHC-II
CD4
Cancer cell
Granzyme B
IFNγ
Macrophage Activation
CD4
IFNγ
CD40L CD40
CD4
TCR MHC-II
Cancer cell
Macrophage
Nitric Oxide
Cytokine Secretion within TME
IL-2
CD8
CD4
Macrophage
IFNγ
TNFα
Cytotoxic Activity
IFNγ
TNFα
IL-12
Cancer cell
Cytotoxic Activity
NK
Tumor Microenvironment

Figure 2: Tracking the development of neoantigen-specific CD4$^+$ T cells against SCC VII in the tumor-draining lymph node.

a. ELISpot response for splenocytes harvested from naive mice or mice vaccinated with 50μg PolyI:C + 100μg of the indicated peptide 14 days prior to the ELISpot. Rechallenge was performed with either no peptide (Negative), the indicated peptide, or Concanvalin A. n=3 for all groups. Data bars represent mean ± s.e.m. All data is from 1 experiment.

b. ELISpot response for splenocytes harvested from naïve mice or mice vaccinated with 50μg PolyI:C + 100μg of Mut_48 14 days prior to the ELISpot and depleted of either CD4+ or CD8+ T cells three days prior to the ELISpot. n=3 for all groups. Data bars represent mean ± s.e.m. All data is from 1 experiment.

c. ELISpot response for splenocytes harvested from naïve mice or mice vaccinated with 50μg PolyI:C and 100μg of either Mut_48 or Mut_48.10 14 days prior to the ELISpot. Indicated mice were also given CD8+ T cell-depleting antibodies. Indicated wells also had 20μg/mL I-A-k blocking antibodies included during the 20 hour incubation prior to plate development. n=3 for all groups. Data bars represent mean ± s.e.m. All data is from 1 experiment.

d. Tumor growth curves for mice receiving PBS (black), 100μg Mut_48 + 50μg PolyI:C + 200μg αPD-1 (red), immune checkpoint blockade alone (blue), or NeoAg vaccination alone (green) starting 6 days after SCC VII tumor challenge. n=5 for all groups. ****p < 0.0001 for Untreated vs Mut_48 + PolyI:C + αPD-1; ns p = 0.2470 for Mut_48 + PolyI:C + αPD-1 vs αPD-1; *p = 0.0434 for Mut_48 + PolyI:C + αPD-1 vs Mut_48 + PolyI:C using two-way ANOVA with Šidák correction for multiple comparisons. n=5 for all groups. Data points represent mean ± s.e.m. All data is from 1 experiment.

e. Tumor growth curves for mice receiving PBS (black) or therapeutic vaccination plus isotype control (red), CD4 depleting antibody (blue), or CD40/CD40L blockade (green) at the indicated time points. n=5 for all groups. ****p < 0.0001 for Untreated vs Mut_48 + PolyI:C + αPD-1; *p = 0.0258 for Mut_48 + PolyI:C + αPD-1 vs Mut_48 + PolyI:C + αPD-1 + CD4 depletion; *p = 0.0386 for Mut_48 + PolyI:C + αPD-1 vs Mut_48 + PolyI:C + αPD-1 + CD40L blockade using two-way ANOVA with Šidák correction for multiple comparisons. n=5 for all groups. Data points represent mean ± s.e.m. All data is from 1 experiment.

f. Representative flow cytometry plots of tetramer gating with clip and CLTCH129>Q/I-Ak tetramers in naïve and tumor-bearing animals to identify CLTCH129>Q-specific CD4+ T cells within the tdLN of tumor-bearing animals. Data from 12 days after tumor inoculation.

g. Quantification of CLTCH129>Q-specific CD4+ T cells in the tumor-draining lymph nodes of mice challenged with SCC VII tumors in untreated mice (black) or mice undergoing therapeutic vaccination (red). ns p=0.1229 for Untreated vs Mut_48 + PolyI:C + αPD-1 12 days after tumor inoculation; **p = 0.0054 for Untreated vs Mut_48 + PolyI:C + αPD-1 18 days after tumor inoculation using t-tests comparing each time point. n=4 for untreated six days after tumor inoculation and Mut_48 + PolyI:C + αPD-1 18 days after tumor inoculation. n=5 for all other points. Data points represent mean ± s.e.m. All data is from 1 experiment.

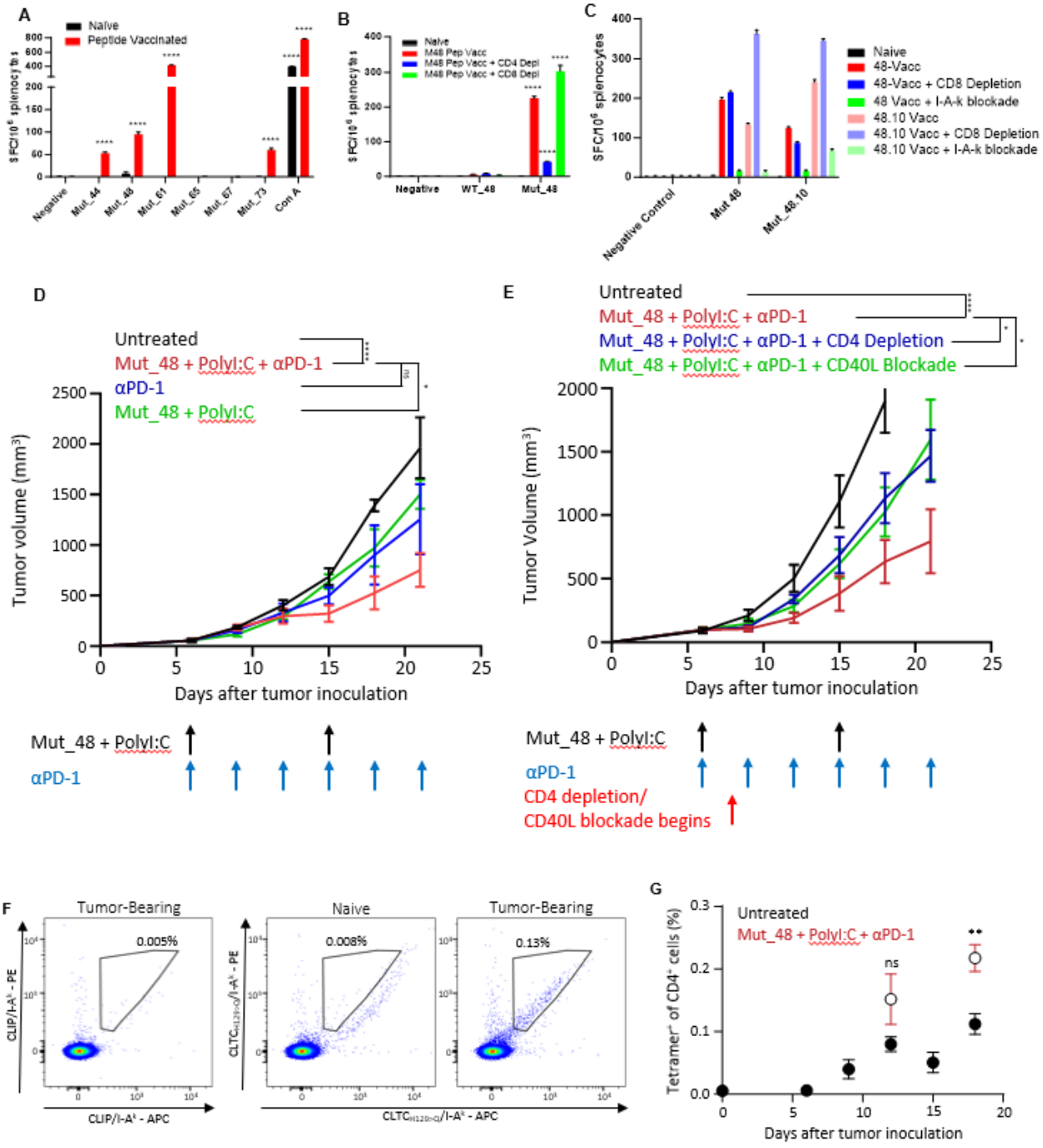

A
Naive
Peptide Vaccinated
Negative
Mut_44
Mut_48
Mut_61
Mut_65
Mut_67
Mut_73
Con A
B
Naive
M48 Pep Vacc
M48 Pep Vacc + CD4 Depl
M48 Pep Vacc + CD8 Depl
Negative
WT_48
Mut_48
C
Naive
48-Vacc
48-Vacc + CD8 Depletion
48 Vacc + I-A-k blockade
48.10 Vacc
48.10 Vacc + CD8 Depletion
48.10 Vacc + I-A-k blockade
Negative Control
Mut 48
Mut_48.10
SFC/10⁶ splenocytes
D
Untreated
Mut_48 + PolyI:C + αPD-1
αPD-1
Mut_48 + PolyI:C
Tumor volume (mm³)
Days after tumor inoculation
Mut_48 + PolyI:C
αPD-1
E
Untreated
Mut_48 + PolyI:C + αPD-1
Mut_48 + PolyI:C + αPD-1 + CD4 Depletion
Mut_48 + PolyI:C + αPD-1 + CD40L Blockade
Tumor Volume (mm³)
Days after tumor inoculation
Mut_48 + PolyI:C
αPD-1
CD4 depletion/
CD40L blockade begins
F
Tumor-Bearing
Naive
Tumor-Bearing
0.005%
0.008%
0.13%
CLIP/I-Aᵏ - PE
CLIP/I-Aᵏ - APC
CLTC(1120-Q)/I-Aᵏ - PE
CLTC(1120-Q)/I-Aᵏ - APC
G
Untreated
Mut_48 + PolyI:C + αPD-1
ns
Tetramer⁺ of CD4⁺ cells (%)
Days after tumor inoculation

Figure 3: Phenotyping the developing CD4$^+$ T cell response against SCC VII in the tumor-draining lymph node.

a. Representative staining showing gating strategies for Th1, Treg, and TfH-like phenotypes as well as PD-1$^+$ and PD-1^{hi} determinations on total (top row) and $CLTC_{H129>Q}$/I-A^k tetramer$^+$ (bottom row) live CD4$^+$ T cells isolating from the tumor-draining lymph node of tumor-bearing animals.

b. Frequencies of CXCR3$^+$, PD-1$^+$, PD-1^{hi}, CXCR5$^+$ PD-1^{hi}, and FoxP3$^+$ cells among total CD4$^+$ T cells in the tumor-draining lymph node throughout tumor growth without treatment (closed circles) or in mice undergoing therapeutic vaccination with Mut_48 + PolyI:C + αPD-1 (open circles), as well as the frequency of PD-1$^+$ cells among FoxP3$^+$ cells. ***p = 0.0005 for CXCR3$^+$; ***p=0.0004 for 12-days post tumor inoculation and ***p=0.0003 for 18-days post tumor inoculation for PD-1$^+$; **p=0.0026 for 12-days post tumor inoculation and **p=0.0027 for 18-days post tumor inoculation for PD-1^{hi}; *p=0.0174 for 12-days post tumor inoculation and **p=0.0044 for 18-days post tumor inoculation for CXCR5$^+$ PD-1^{hi}, **p = 0.0036 for FoxP3$^+$; and **p= 0.0028 for PD-1$^+$ of FoxP3$^+$ using t-tests for each time point. n=5 for all groups. Data points represent mean ± s.e.m. All data is from 1 experiment.

c. Frequencies of CXCR3$^+$, PD-1$^+$, and PD-1^{hi}, CXCR5$^+$ PD-1^{hi}, FoxP3$^+$ cells among $CLTC_{H129>Q}$-specific CD4+ T cells in the tumor-draining lymph node throughout tumor growth without treatment (closed circles) or in mice undergoing therapeutic vaccination with Mut_48 + PolyI:C + αPD-1 (open circles), as well as the frequency of PD-1$^+$ cells among FoxP3$^+$ cells. *p = 0.0211 for CXCR3$^+$; ****p<0.0001 for PD-1$^+$; **p=0.0063 for PD-1^{hi}; ns p=0.0841 for CXCR5$^+$ PD-1^{hi}, *p = 0.0331 for FoxP3$^+$; ns p = .0572 and **p= 0.002 for PD-1$^+$ of FoxP3$^+$ using t-tests for each time point. n=4 for untreated 9 days after tumor inoculation. n=5 for all other points. Data points represent mean ± s.e.m. All data is from 1 experiment.

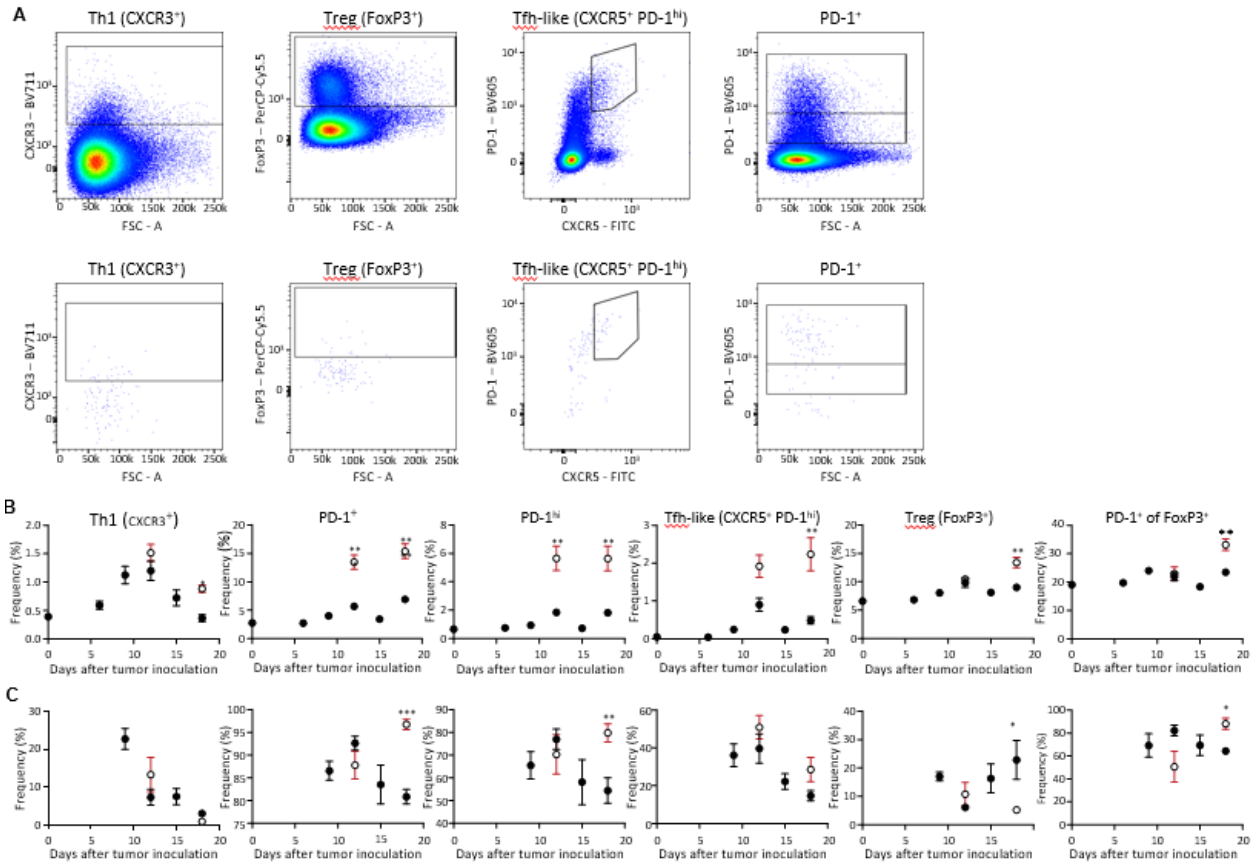

A
Th1 (CXCR3⁺)
Treg (FoxP3⁺)
Tfh-like (CXCR5⁺ PD-1ʰⁱ)
PD-1⁺
CXCR3 – BV711
FoxP3 – PerCP-Cy5.5
PD-1 – BV605
CXCR5 - FITC
FSC - A
B
Th1 (CXCR3⁺)
PD-1⁺
PD-1ʰⁱ
Tfh-like (CXCR5⁺ PD-1ʰⁱ)
Treg (FoxP3⁺)
PD-1⁺ of FoxP3⁺
Frequency (%)
Days after tumor inoculation
C
Frequency (%)
Days after tumor inoculation

Figure 4: Phenotyping tumor-infiltrating $CD4^+$ T cells in SCC VII.

All figures compare untreated (closed circles) to animals undergoing therapeutic vaccination with Mut_48, PolyI:C, and αPD-1 as indicated in Figure 2D/Figure 2E (open circles). All data is from 1 experiment.

a. Quantification of the frequency of $CD4^+$ T cells as a percent of all live $CD45^+$ cells isolated from the TME at the given time points. *p = 0.434; ns p = 0.3458 using one-way ANOVA with Tukey's correction for multiple comparisons. Bars represent mean ± s.e.m.

b. Quantification of $CLTC_{H129>Q}$-specific $CD4^+$ T cells as a percent of tumor-infiltrating $CD4^+$ T cells at the given time points. ns p = 0.3863; *p = 0.0458 using one-way ANOVA with Tukey's correction for multiple comparisons. Bars represent mean ± s.e.m.

c. Frequencies of total $CD4^+$ cells within the tumor that are $CXCR3^+$, $PD\text{-}1^+$, $PD\text{-}1^{hi}$, $CXCR5^+$ $PD\text{-}1^{hi}$, $FoxP3^+$, and $PD\text{-}1^+$ among $Foxp3^+$ 12- and 18-days after tumor inoculation. *p = 0.0453 for $CXCR3^+$; ****p<0.0001 for $PD\text{-}1^{hi}$; **p=0.0044 for $FoxP3^+$; *p= 0.0448 and **p = 0.0029 for $PD\text{-}1^+$ of $FoxP3^+$ using t-tests. Bars represent mean ± s.e.m. d. Frequencies of $CLTC_{H129>Q}$-specific $CD4^+$ T cells within the tumor that are $CXCR3^+$, $PD\text{-}1^+$, $PD\text{-}1^{hi}$, $CXCR5^+$ $PD\text{-}1^{hi}$, $FoxP3^+$, and $PD\text{-}1^+$ among $Foxp3^+$ 18-days after tumor inoculation. *p = 0.0113 for $FoxP3^+$ using t-tests. Bars represent mean ± s.e.m.

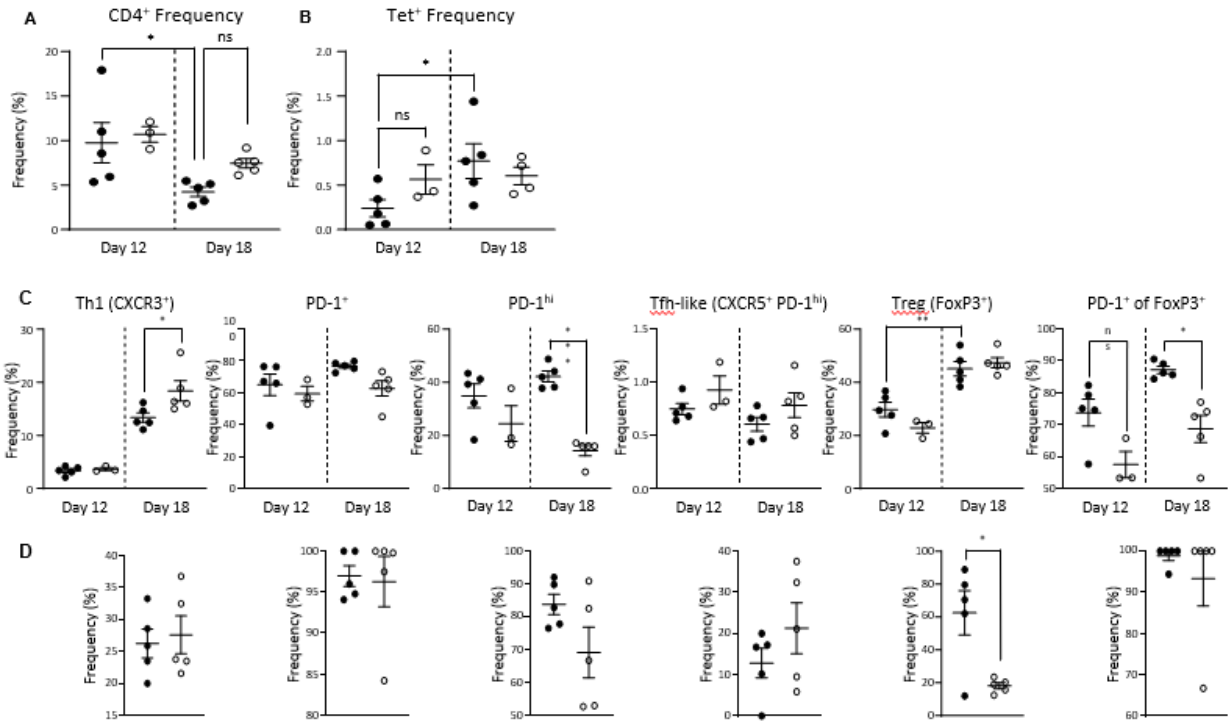

A
CD4⁺ Frequency
B
Tet⁺ Frequency
Frequency (%)
Day 12
Day 18
ns
C
Th1 (CXCR3⁺)
PD-1⁺
PD-1hi
Tfh-like (CXCR5⁺ PD-1hi)
Treg (FoxP3⁺)
PD-1⁺ of FoxP3⁺
D

Figure 5: Investigating the clonality and genetic profile of the neoantigen-specific $CD4^+$ T cell response using single cell genomics.

a. Schematic overview and flow cytometry plots of tetramer sorting experiment to isolate $CLTC_{H129>Q}$-specific $CD4^+$ T cells from tumor-draining lymph nodes (top) plus tetramer staining used to sort tetramer-negative and tetramer-positive cells for further analysis.

b. The UMAP of $CLTC_{H129>Q}$/I-A^k tetramer positive (blue) and tetramer negative (pink) cells determined by Seurat-based clustering. There were a total of 1,581 cells, 432 of which are tetramer-positive and 1,149 of which are tetramer-negative.

c. The UMAP of tetramer positive cells as determined by Seurat-based clustering. (left). A total of 5 clusters (clusters 0-4) were identified and color-coded.

d. The average expression of subset-defining and functional genes by cluster pictured in panel c.

e. TCR Vβ gene diversity from sorted $CLTC_{H129>Q}$/I-A^k tetramer negative and tetramer positive cells.

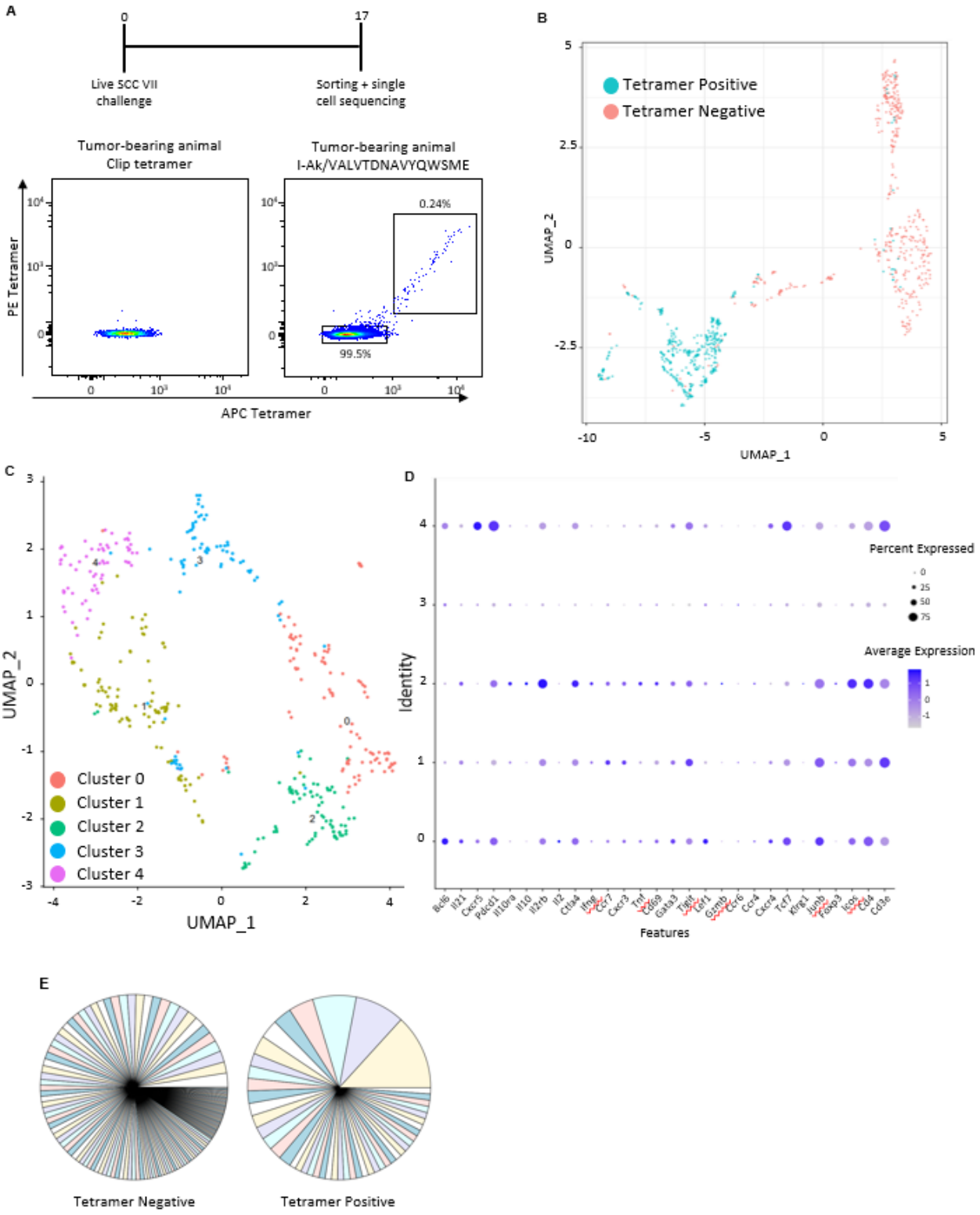

A
0
17
Live SCC VII challenge
Sorting + single cell sequencing
Tumor-bearing animal Clip tetramer
Tumor-bearing animal I-Ak/VALVTDNAVYQWSME
PE Tetramer
APC Tetramer
0.24%
99.5%
B
Tetramer Positive
Tetramer Negative
UMAP_2
UMAP_1
C
Cluster 0
Cluster 1
Cluster 2
Cluster 3
Cluster 4
UMAP_2
UMAP_1
D
Percent Expressed
Average Expression
Identity
Features
Bcl6 Il21 Cxcr5 Pdcd1 Il10ra Il10 Il2rb Il2 Ctla4 Ifng Ccr7 Cxcr3 Tnf Cd69 Gata3 Tbx21 Lef1 Gzmb Ccr6 Ccr4 Cxcr4 Tcf7 Klrg1 Junb Foxp3 Icos Cd4 Cd3e
E
Tetramer Negative
Tetramer Positive

Figure 6: Characterizing the clonality and phenotypes of $CLTC_{H129>Q}$-specific TCRs.

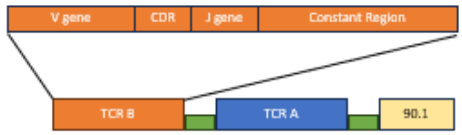
a. Schematic construct for retroviral production and transfection containing TCR genes of interest alongside CD90.1.

b. Flow cytometry plots demonstrating the expression of the transduced TCR Vβ gene and CD90.1 in primary mouse CD4+ T cells after a mock transduction (left) or with a TCR of interest following a low (middle) or high (right) efficiency transduction.

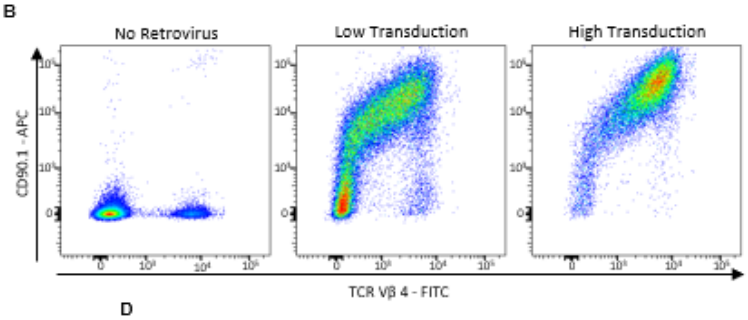
c. The UMAP of tetramer positive cells as determined by Seurat-based clustering with clones verified by TCR expression and tetramer binding highlighted.

d. Quantification of the number of cells for each clone within the given clusters determined in figure 5c and figure 5d.

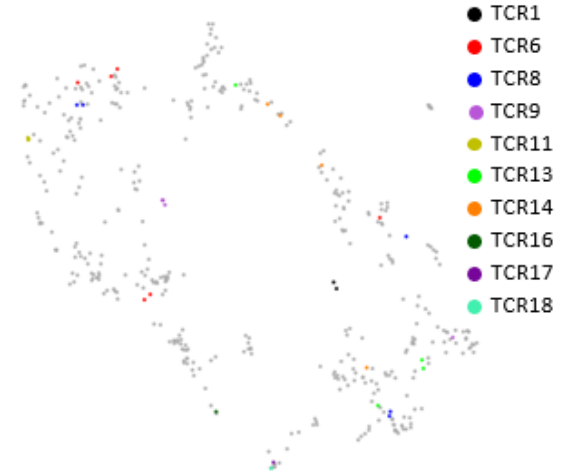
A



B



C



D

Identifier	Th1	TfH	Regulatory	Stem-Like	Other
TCR1				2	
TCR2		1	3		
TCR6	2	3			
TCR8	2		2	1	
TCR9		3		1	
TCR11		3			
TCR13			1	2	1
TCR14			1	1	2
TCR16			1		
TCR17			1		
TCR18			1		

Figure 7: Expression and characterization of neoantigen-specific TCRs.

a. Flow cytometry plots showcasing the titration of $CLTC_{H129>Q}/I\text{-}A^{k}$ tetramer on two different TCRs with similar affinities.

b. Quantification of tetramer affinity of validated neoantigen-specific TCRs normalized using CD90.1 over the range of concentrations tested during titration. Data points represent mean ± s.e.m. from 3 experiments.

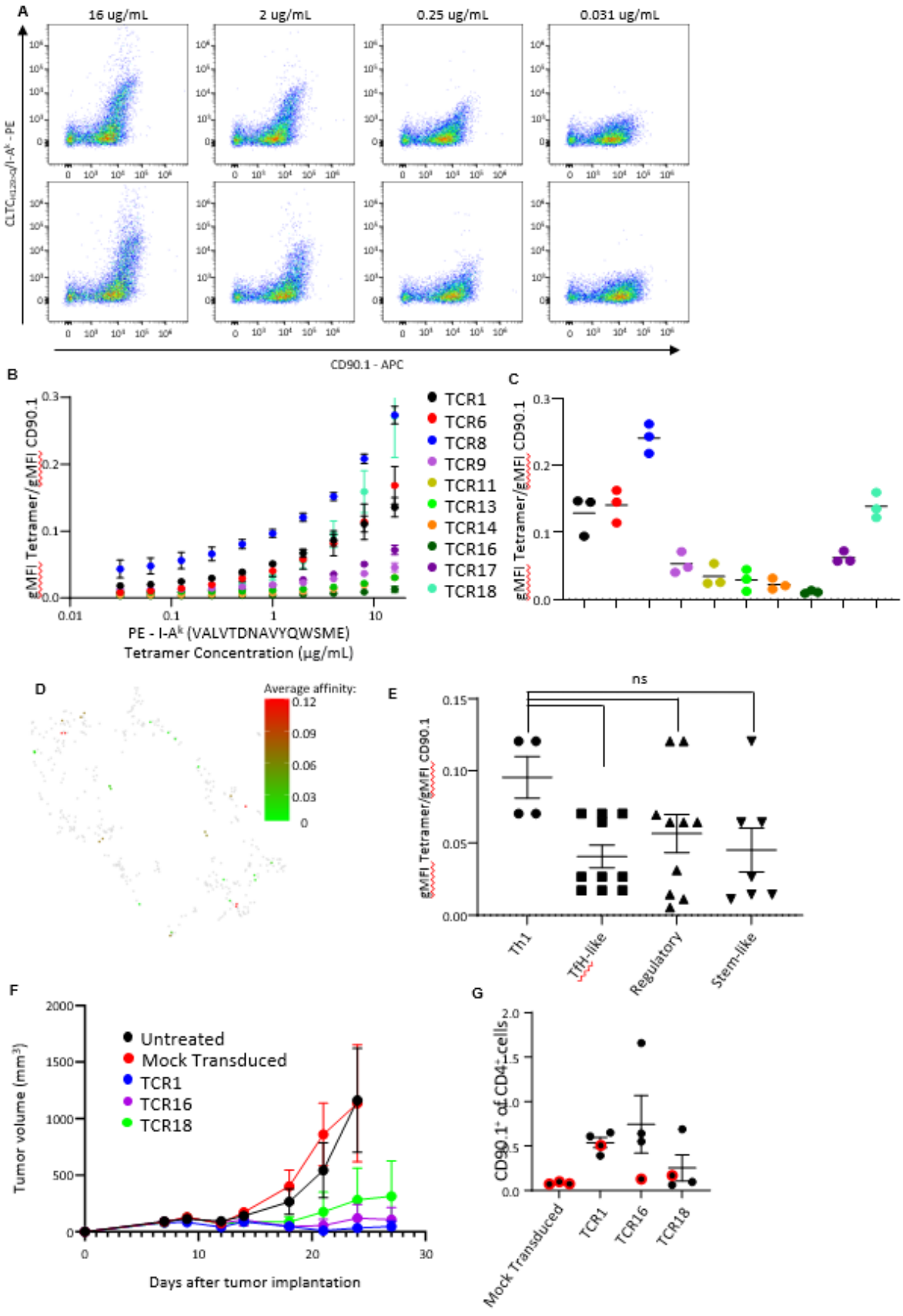
c. Quantification of normalized tetramer affinity for validated neoantigen-specific TCRs at a concentration of 2ug/mL used throughout figures 1, 2, and 3. Data points represent mean ± s.e.m. from 3 experiments.

d. Heat map of normalized tetramer affinity determined in figure 7c overlaid on the UMAP seen in figure 5c.

e. Quantification of TCR affinity for clones within each of the phenotypic clusters determined in figure 5c. p = 0.0628 for Th1 vs TfH-like; p = 0.2660 for Th1 vs Regulatory; p = 0.1276 for Th1 vs Stem-like using one-way Anova. Bars represent mean ± s.e.m.

f. Tumor growth curves for mice that received cyclophosphamide seven days post tumor inoculation and either PBS (Black) or 3×10^{6} adoptively transferred $CD4^{+}$ T cells following mock transduction (red) or transduced to express STCR1 (blue), TCR16 (purple), or TCR18 (green) eight days after tumor inoculation. ***p = 0.0007 for Mock Transduced vs TCR1; **p = 0.0033 for Mock Transduced vs TCR16; *p = 0.0352 for Mock Transduced vs TCR15 using two-way ANOVA with Šidák correction for multiple comparisons. n=4 for all points. Data points represent mean ± s.e.m.

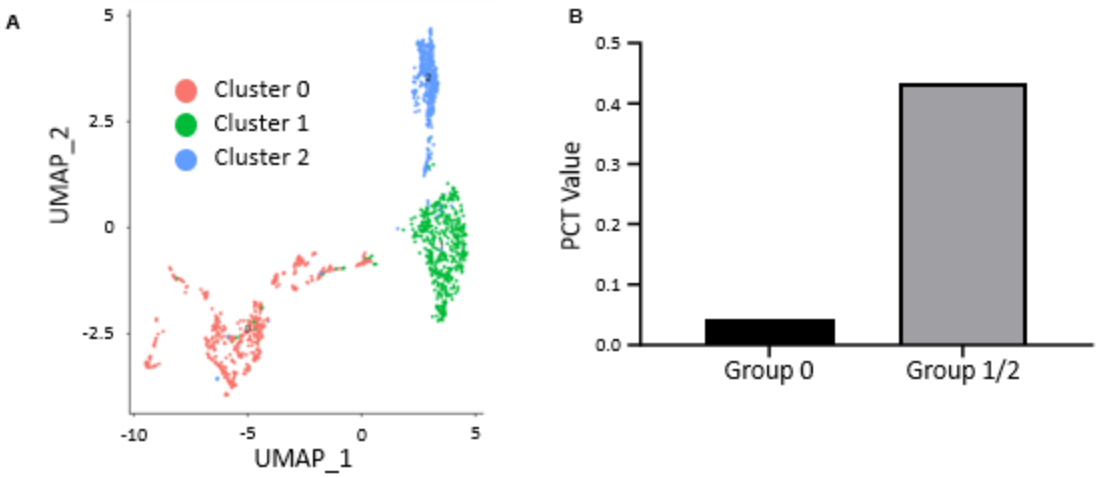
g. Frequency of $CD90.1^{+}$ cells as a percent of all $CD4^{+}$ T cells found within the tumor-draining lymph node 27 days post tumor inoculation. Red outlines indicate animals with active tumor. Bars represent mean ± s.e.m.


A
16 ug/mL
2 ug/mL
0.25 ug/mL
0.031 ug/mL
CLTC(1125-Q)/I-Ak - PE
CD90.1 - APC
B
gMFI Tetramer/gMFI CD90.1
PE - I-Ak (VALVTDNAVYQWSME)
Tetramer Concentration (µg/mL)
TCR1
TCR6
TCR8
TCR9
TCR11
TCR13
TCR14
TCR16
TCR17
TCR18
C
gMFI Tetramer/gMFI CD90.1
D
Average affinity:
0.12
0.09
0.06
0.03
0
E
ns
gMFI Tetramer/gMFI CD90.1
Th1
Tfh-like
Regulatory
Stem-like
F
Tumor volume (mm3)
Days after tumor implantation
Untreated
Mock Transduced
TCR1
TCR16
TCR18
G
CD90.1+ of CD4+ cells
Mock Transduced
TCR1
TCR16
TCR18

Supplemental Figure 1: Different activation states for total and CLTC$_{H129>Q}$-specific cells.

a. UMAP with grouping based on activation states determined by Seurat-based clustering originally pictured in figure 5b. Group 0 is primarily composed of tetramer negative cells while groups 1 and 2 are composed of tetramer positive cells.

b. Relative CD44 expression of the three groups seen in panel **a.**


A
Cluster 0
Cluster 1
Cluster 2
UMAP_2
UMAP_1
5
2.5
0
-2.5
-10
-5
0
5
B
PCT Value
0.5
0.4
0.3
0.2
0.1
0.0
Group 0
Group 1/2

Supplemental Figure 2: Transduction efficiency of adoptively transferred cells.

a. CD90.1 expression versus tetramer binding for the four adoptively transferred cells prior to injection 8 days post tumor inoculation used in figures 6f and 6g.

A

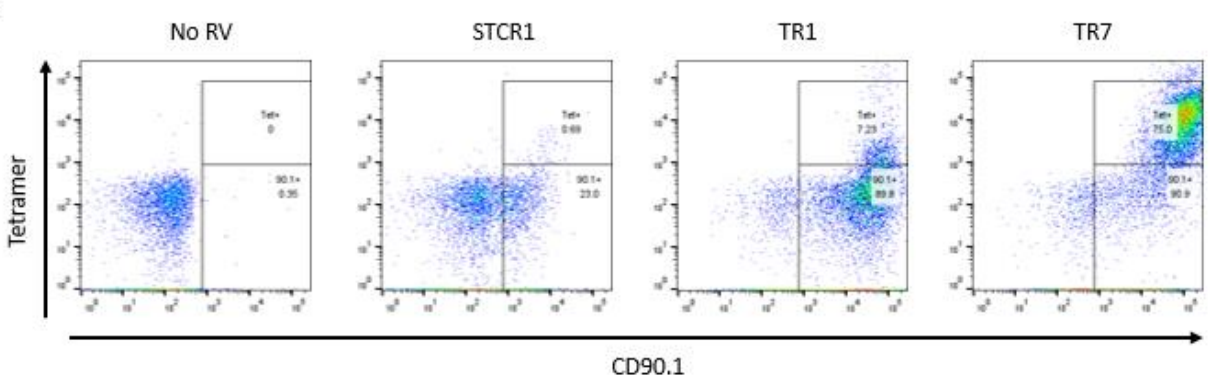


Table 1: List of the TCRs of interest

Clone ID	Clone #	TRAV	TRAJ	TRBV	TRBJ
TCR1	2	TRAV9-4	TRAJ5	TRBV13-1	TRBJ1-1
TCR2	5	TRAV9-4	TRAJ5	TRBV13-1	TRBJ1-1
TCR3	11	TRAV13-4-DV7	TRAJ27	TRBV10	TRBJ1-4
TCR4	9	TRAV14D-1	TRAJ21	TRBV13-3	TRBJ1-2
TCR5	8	TRAV4-2	TRAJ26	TRBV1	TRBJ2-5
TCR6	6	TRAV7D-5	TRAJ15	TRBV2	TRBJ1-5
TCR7	6	TRAV7D-4	TRAJ7	TRBV5	TRBJ2-5
TCR8	5	TRAV7-1	TRAJ37	TRBV2	TRBJ2-5
TCR9	5	TRAV6D-4	TRAJ43	TRBV12-2 + TRBV13-2	TRBJ1-4
TCR10	5	TRAV3-4	TRAJ40	TRBV12-2 + TRBV13-2	TRBJ2-7
TCR11	4	TRAV7D-5	TRAJ37	TRBV2	TRBJ2-1
TCR12	4	TRAV14D-1	TRAJ21	TRBV13-3	TRBJ1-4
TCR13	4	TRAV14D-2	TRAJ9	TRBV31	TRBJ1-3
TCR14	4	TRAV4-3	TRAI9	TRBV1	TRABJ1-3
TCR15	5	TRAV14D-2	TRAJ40	TRBV1	TRBJ2-7
TCR16	1	TRAV6N-7	TRAJ57	TRBV2	TRBJ2-7
TCR17	1	TRAV7-1	TRAJ37	TRBV2	TRBJ2-7
TCR18	1	TRAV7-3	TRAJ15	TRBV2	TRBJ2-7
TCR19	7	TRAV4-2	TRAJ37	TRBV20	TRBJ1-6
TCR20	6	TRAV6-2	TRAJ6	TRBV20	TRBJ2-7

Table 2: Ability of each TCR to be expressed and bind tetramer

Clone ID	Clone #	CD90.1 Expression	Tetramer Binding
TCR1	2	Yes	Yes
TCR2	5	Yes	Yes
TCR3	11	Yes	No
TCR4	9	Yes	No
TCR5	8	Yes	No
TCR6	6	Yes	Yes
TCR7	6	Yes	No
TCR8	5	Yes	Yes
TCR9	5	Yes	Yes
TCR10	5	Yes	No
TCR11	4	Yes	Yes
TCR12	4	No	No
TCR13	4	Yes	Yes
TCR14	4	Yes	Yes
TCR15	5	Yes	No
TCR16	1	Yes	Yes
TCR17	1	Yes	Yes
TCR18	1	Yes	Yes
TCR19	7	Yes	No
TCR20	6	Yes	No

REFERENCES

1. Homma, S., Komita, H., Sagawa, Y., Ohno, T. & Toda, G. Antitumour activity mediated by CD4+ cytotoxic T lymphocytes against MHC class II-negative mouse hepatocellular carcinoma induced by dendritic cell vaccine and interleukin-12. *Immunology* **115**, 451–461 (2005).

2. Lu, Y. *et al.* Th9 Cells Represent a Unique Subset of CD4+ T Cells Endowed with the Ability to Eradicate Advanced Tumors. *Cancer Cell* **33**, 1048-1060.e7 (2018).

3. Kravtsov, D. S., Erbe, A. K., Sondel, P. M. & Rakhmilevich, A. L. Roles of CD4+ T cells as mediators of antitumor immunity. *Frontiers in Immunology* vol. 13 Preprint at https://doi.org/10.3389/fimmu.2022.972021 (2022).

4. Haen, S. P., Löffler, M. W., Rammensee, H. G. & Brossart, P. Towards new horizons: characterization, classification and implications of the tumour antigenic repertoire. *Nature Reviews Clinical Oncology* vol. 17 595–610 Preprint at https://doi.org/10.1038/s41571-020-0387-x (2020).

5. Lee, C. H., Yelensky, R., Jooss, K. & Chan, T. A. Update on Tumor Neoantigens and Their Utility: Why It Is Good to Be Different. *Trends in Immunology* vol. 39 536–548 Preprint at https://doi.org/10.1016/j.it.2018.04.005 (2018).

6. Leko, V. & Rosenberg, S. A. Identifying and Targeting Human Tumor Antigens for T Cell-Based Immunotherapy of Solid Tumors. *Cancer Cell* vol. 38 454–472 Preprint at https://doi.org/10.1016/j.ccell.2020.07.013 (2020).

7. Higgins, J. P., Bernstein, M. B. & Hodge, J. W. Enhancing immune responses to tumor-associated antigens. *Cancer Biology and Therapy* vol. 8 Preprint at https://doi.org/10.4161/cbt.8.15.9133 (2009).

8. Cattaneo, C. M. *et al.* Identification of patient-specific CD4+ and CD8+ T cell neoantigens through HLA-unbiased genetic screens. *Nat Biotechnol* **41**, 783–787 (2023).

9. Dong, M. B. *et al.* Systematic Immunotherapy Target Discovery Using Genome-Scale In Vivo CRISPR Screens in CD8 T Cells. *Cell* **178**, 1189-1204.e23 (2019).

10. He, X. *et al.* An In Vivo Screen to Identify Short Peptide Mimotopes with Enhanced Antitumor Immunogenicity. *Cancer Immunol Res* **10**, 314–326 (2022).

11. Bandlamudi, C., Razavi, P., Wen, H. Y., Weigelt, B. & Zumbo, P. Immunogenicity and therapeutic targeting of a public neoantigen derived from mutated. doi:10.1038/s41591-022-01786-3.

12. Nibeyro, G. *et al.* Unraveling tumor specific neoantigen immunogenicity prediction: a comprehensive analysis. *Front Immunol* **14**, (2023).

13. Xu, S., Wang, X. & Fei, C. A Highly Effective System for Predicting MHC-II Epitopes With Immunogenicity. *Front Oncol* **12**, (2022).

14. Moore, T. V. & Nishimura, M. I. Improved MHC II epitope prediction - a step towards personalized medicine. *Nature reviews. Clinical oncology* vol. 17 71–72 Preprint at https://doi.org/10.1038/s41571-019-0315-0 (2020).

15. Vyasamneni, R. *et al.* A universal MHCII technology platform to characterize antigen-specific CD4+ T cells. *Cell Reports Methods* **3**, (2023).

16. De Mattos-Arruda, L. *et al.* Neoantigen prediction and computational perspectives towards clinical benefit: recommendations from the ESMO Precision Medicine Working Group. *Annals of Oncology* vol. 31 978–990 Preprint at https://doi.org/10.1016/j.annonc.2020.05.008 (2020).

17. Barra, C. *et al.* Footprints of antigen processing boost MHC class II natural ligand predictions. *Genome Med* **10**, (2018).

18. De Mattos-Arruda, L. *et al.* Neoantigen prediction and computational perspectives towards clinical benefit: recommendations from the ESMO Precision Medicine Working Group. *Annals of Oncology* vol. 31 978–990 Preprint at https://doi.org/10.1016/j.annonc.2020.05.008 (2020).

19. Schumacher, T. N. & Schreiber, R. D. *Neoantigens in Cancer Immunotherapy*. www.sciencemag.org.

20. Schrieber. MHC-II neoantigens shape tumor immunity and response to immunotherapy.

21. Ward, J. P., Gubin, M. M. & Schreiber, R. D. The Role of Neoantigens in Naturally Occurring and Therapeutically Induced Immune Responses to Cancer. in *Advances in Immunology* vol. 130 25–74 (Academic Press Inc., 2016).

22. Spencer, S. Harnessing neoantigen specific CD4 T cells for cancer immunotherapy. Preprint at (2020).

23. Puig-Saus, C. *et al.* Neoantigen-targeted CD8+ T cell responses with PD-1 blockade therapy. *Nature* (2023) doi:10.1038/s41586-023-05787-1.

24. Cui, C. *et al.* Neoantigen-driven B cell and CD4 T follicular helper cell collaboration promotes anti-tumor CD8 T cell responses. *Cell* 1–18 (2021) doi:10.1016/j.cell.2021.11.007.

25. Zhou, W., Yu, J., Li, Y. & Wang, K. Neoantigen-specific TCR-T cell-based immunotherapy for acute myeloid leukemia. *Exp Hematol Oncol* **11**, 1–15 (2022).

26. Peri, A. *et al.* The landscape of T cell antigens for cancer immunotherapy. *Nature Cancer* vol. 4 937–954 Preprint at https://doi.org/10.1038/s43018-023-00588-x (2023).

27. Jordanova, E. S. *et al.* Human leukocyte antigen class I, MHC class I chain-related molecule A, and CD8+/regulatory T-cell ratio: Which variable determines survival of cervical cancer patients? *Clinical Cancer Research* **14**, 2028–2035 (2008).

28. Brightman, S. E. *et al.* Neoantigen-specific stem cell memory-like CD4+ T cells mediate CD8+ T cell-dependent immunotherapy of MHC class II-negative solid tumors. *Nat Immunol* **24**, 1345–1357 (2023).

29. Speiser, D. E., Chijioke, O., Schaeuble, K. & Münz, C. CD4+ T cells in cancer. *Nat Cancer* **4**, 317–329 (2023).

30. Frangione, V., Mortara, L., Castellani, P., De Lerma Barbaro, A. & Accolla, R. S. CIITA-driven MHC-II positive tumor cells: Preventive vaccines and superior generators of antitumor CD4+ T lymphocytes for immunotherapy. *Int J Cancer* **127**, 1614–1624 (2010).

31. Quezada, S. A. *et al.* Tumor-reactive CD4+ T cells develop cytotoxic activity and eradicate large established melanoma after transfer into lymphopenic hosts. *Journal of Experimental Medicine* **207**, 637–650 (2010).

32. Brightman, S. E. *et al.* Tumor cells fail to present MHC-II-restricted epitopes derived from oncogenes to CD4 + T cells. (2023) doi:10.1172/jci.

33. Axelrod, M. L., Cook, R. S., Johnson, D. B. & Balko, J. M. Biological consequences of MHC-II expression by tumor cells in cancer. *Clinical Cancer Research* vol. 25 2392–2402 Preprint at https://doi.org/10.1158/1078-0432.CCR-18-3200 (2019).

34. M Toes U, R. E., Schoenberger, S. P., H van der Voort U, E. I., Rienk, O. & M Melief U, C. J. *CD40-CD40Ligand Interactions and Their Role in Cytotoxic T Lymphocyte Priming and Anti-Tumor Immunity Cross-Presentation of Antigens Can Lead Both to Priming and Tolerization of CTL*. *seminars in I MMU NOLOGY* vol. 10 (1998).

35. Schoenberger, S. P., Toes, R. E., van der Voort, E. I., Offringa, R. & Melief, C. J. T-cell help for cytotoxic T lymphocytes is mediated by CD40-CD40L interactions. *Nature* **393**, 480–483 (1998).

36. Ma, D. Y. & Clark, E. A. The role of CD40 and CD154/CD40L in dendritic cells. *Seminars in Immunology* vol. 21 265–272 Preprint at https://doi.org/10.1016/j.smim.2009.05.010 (2009).

37. Richman, L. P. & Vonderheide, R. H. Role of crosslinking for agonistic CD40 monoclonal antibodies as immune therapy of cancer. **2**, 1–12 (2015).

38. Kuhn, N. F. *et al.* CD40 Ligand-Modified Chimeric Antigen Receptor T Cells Enhance Antitumor Function by Eliciting an Endogenous Antitumor Response. *Cancer Cell* **35**, 473-488.e6 (2019).

39. Watanabe, M. *et al.* Co-stimulatory function in primary germinal center responses : CD40 and B7 are required on distinct antigen- presenting cells The Journal of Experimental Medicine. 2795–2810 (2017).

40. Xu, A. *et al.* CD40 agonist converting CTL exhaustion via the activation of the mTORC1 pathway enhances PD-1 antagonist action in rescuing exhausted CTLs in chronic infection. *Biochem Biophys Res Commun* **484**, 662–667 (2017).

41. Poncette, L., Bluhm, J. & Blankenstein, T. The role of CD4 T cells in rejection of solid tumors. *Current Opinion in Immunology* vol. 74 18–24 Preprint at https://doi.org/10.1016/j.coi.2021.09.005 (2022).

42. Kotov, D. I. *et al.* TCR Affinity Biases Th Cell Differentiation by Regulating CD25, Eef1e1, and Gbp2. *The Journal of Immunology* ji1801609 (2019) doi:10.4049/jimmunol.1801609.

43. Inoshima, I. *et al.* T Cell Receptor Signaling in the Control of Regulatory T Cell Differentiation and Function. **17**, 1310–1314 (2012).

44. Fahey, L. M. *et al.* Viral persistence redirects CD4 T cell differentiation toward T follicular helper cells. *Journal of Experimental Medicine* **208**, 987–999 (2011).

45. Zhu, J., Yamane, H. & Paul, W. E. Differentiation of effector CD4+ T cell populations. *Annual Review of Immunology* vol. 28 445–489 Preprint at https://doi.org/10.1146/annurev-immunol-030409-101212 (2010).

46. Zhu, X. & Zhu, J. CD4 T helper cell subsets and related human immunological disorders. *International Journal of Molecular Sciences* vol. 21 1–26 Preprint at https://doi.org/10.3390/ijms21218011 (2020).

47. Golubovskaya, V. & Wu, L. Different subsets of T cells, memory, effector functions, and CAR-T immunotherapy. *Cancers* vol. 8 Preprint at https://doi.org/10.3390/cancers8030036 (2016).

48. Sun, L. *et al.* Interleukin 12 (IL-12) Family Cytokines: Role in Immune Pathogenesis and Treatment of CNS Autoimmune Disease Lin. **75**, 249–255 (2016).

49. Kim, M. T., Harty, J. T., Cd, E. & Response, T. C. Impact of inflammatory cytokines on effector and memory CD8 + T cells. **5**, 1–5 (2014).

50. Onur Boyman, 1 Marek Kovar, 1 Mark P. Rubinstein, 1 Charles D. Surh, 1 Jonathan Sprent. Selective Stimulation of T Cell subsets with antibody-cytokine immune complexes. **1924**, 1924–1928 (2010).

51. Parihar, R., Dierksheide, J., Hu, Y. & Carson, W. E. IL-12 enhances the natural killer cell cytokine response to Ab-coated tumor cells. *Journal of Clinical Investigation* **110**, 983–992 (2002).

52. Eftychi, C. *et al.* Temporally Distinct Functions of the Cytokines IL-12 and IL-23 Drive Chronic Colon Inflammation in Response to Intestinal Barrier Impairment. *Immunity* 1–14 (2019) doi:10.1016/j.immuni.2019.06.008.

53. Komuczki, J. *et al.* Fate-Mapping of GM-CSF Expression Identifies a Discrete Subset of Inflammation-Driving T Helper Cells Regulated by Cytokines IL-23 and IL-1β. *Immunity* 1–16 (2019) doi:10.1016/j.immuni.2019.04.006.

54. Vacaflores, A., Chapman, N. M., Harty, J. T., Richer, M. J. & Jon, C. Exposure of Human CD4 T Cells to IL-12 Results in Enhanced TCR-Induced Cytokine Production , Altered TCR Signaling , and Increased Oxidative Metabolism. 1–24 (2016) doi:10.1371/journal.pone.0157175.

55. (LJI), S. C. T follicular helper cell differntiation, function, and roles in disease. *J immunology* **24**, 157–160 (2014).

56. Baumjohann, D. & Brossart, P. T follicular helper cells: Linking cancer immunotherapy and immune-related adverse events. *J Immunother Cancer* **9**, 1–4 (2021).

57. Ise, W. *et al.* T Follicular Helper Cell-Germinal Center B Cell Interaction Strength Regulates Entry into Plasma Cell or Recycling Germinal Center Cell Fate. *Immunity* **48**, 702-715.e4 (2018).

58. Ann L Coker & Nalawansha, Dhanusha A. Pflum, M. K. TfH cell biology: A decade of discovery and diseases. *Physiol Behav* **176**, 139–148 (2019).

59. Kinker, G. S. *et al.* B Cell Orchestration of Anti-tumor Immune Responses: A Matter of Cell Localization and Communication. *Frontiers in Cell and Developmental Biology* vol. 9 Preprint at https://doi.org/10.3389/fcell.2021.678127 (2021).

60. Niogret, J. *et al.* Follicular helper-T cells restore CD8 + -dependent antitumor immunity and anti-PD-L1/PD-1 efficacy. *J Immunother Cancer* **9**, 1–16 (2021).

61. Poultsidi, A. *et al.* Lymph Node Cellular Dynamics in Cancer and HIV: What Can We Learn for the Follicular CD4 (Tfh) Cells? *Front Immunol* **9**, 1–12 (2018).

62. Schmidleithner, L. & Feuerer, M. Tfh cells induce intratumoral tertiary lymphoid structures. *Trends Immunol* **43**, 274–276 (2022).

63. Sun, Q. *et al.* Immune checkpoint therapy for solid tumours: clinical dilemmas and future trends. *Signal Transduction and Targeted Therapy* vol. 8 Preprint at https://doi.org/10.1038/s41392-023-01522-4 (2023).

64. Chocarro, L. *et al.* Cutting-Edge: Preclinical and Clinical Development of the First Approved Lag-3 Inhibitor. *Cells* vol. 11 Preprint at https://doi.org/10.3390/cells11152351 (2022).

65. Popp, F. C. *et al.* Expression of immune checkpoint regulators ido, vista, lag3, and tim3 in resected pancreatic ductal adenocarcinoma. *Cancers (Basel)* **13**, (2021).

66. Deng, J. *et al.* OX40 (CD134) and OX40 ligand, important immune checkpoints in cancer. *Onco Targets Ther* **12**, 7347–7353 (2019).

67. Singh, R., Kim, Y. H., Lee, S. J., Eom, H. S. & Choi, B. K. 4-1BB immunotherapy: advances and hurdles. *Experimental and Molecular Medicine* Preprint at https://doi.org/10.1038/s12276-023-01136-4 (2024).

68. Wang, Y. T. *et al.* Targeting 4-1BB for tumor immunotherapy from bench to bedside. *Frontiers in Immunology* vol. 13 Preprint at https://doi.org/10.3389/fimmu.2022.975926 (2022).

69. Tang, W., Chen, J., Ji, T. & Cong, X. TIGIT, a novel immune checkpoint therapy for melanoma. *Cell Death and Disease* vol. 14 Preprint at https://doi.org/10.1038/s41419-023-05961-3 (2023).

70. Alkhayyal, N. *et al.* Expression of immune checkpoints (PD-L1 and IDO) and tumour-infiltrating lymphocytes in breast cancer. *Heliyon* **8**, (2022).

71. He, Y. *et al.* TIM-3, a promising target for cancer immunotherapy. *OncoTargets and Therapy* vol. 11 7005–7009 Preprint at https://doi.org/10.2147/OTT.S170385 (2018).

72. Solinas, C., Gu-Trantien, C. & Willard-Gallo, K. The rationale behind targeting the ICOS-ICOS ligand costimulatory pathway in cancer immunotherapy. *ESMO Open* vol. 5 Preprint at https://doi.org/10.1136/esmoopen-2019-000544 (2020).

73. Allard, D., Allard, B. & Stagg, J. On the mechanism of anti-CD39 immune checkpoint therapy. *Journal for ImmunoTherapy of Cancer* vol. 8 Preprint at https://doi.org/10.1136/jitc-2019-000186 (2020).

74. Yin, Q. *et al.* Immune-related adverse events of immune checkpoint inhibitors: a review. *Frontiers in Immunology* vol. 14 Preprint at https://doi.org/10.3389/fimmu.2023.1167975 (2023).

75. Park, J. A. & Cheung, N. K. V. Limitations and opportunities for immune checkpoint inhibitors in pediatric malignancies. *Cancer Treatment Reviews* vol. 58 22–33 Preprint at https://doi.org/10.1016/j.ctrv.2017.05.006 (2017).

76. Dobosz, P., Stępień, M., Golke, A. & Dzieciątkowski, T. Challenges of the Immunotherapy: Perspectives and Limitations of the Immune Checkpoint Inhibitor Treatment. *International Journal of Molecular Sciences* vol. 23 Preprint at https://doi.org/10.3390/ijms23052847 (2022).

77. Rizvi, N. A. *et al.* Mutational landscape determines sensitivity to PD-1 blockade in non-small cell lung cancer. *Science (1979)* **348**, 124–128 (2015).

78. Le, D. T. *et al.* PD-1 Blockade in Tumors with Mismatch-Repair Deficiency. *New England Journal of Medicine* **372**, 2509–2520 (2015).

79. Gubin, M. M. *et al.* Checkpoint blockade cancer immunotherapy targets tumour-specific mutant antigens. *Nature* **515**, 577–581 (2014).

80. Alspach, E. *et al.* MHC-II neoantigens shape tumour immunity and response to immunotherapy. *Nature* **574**, 696–701 (2019).

81. McGranahan, N. *et al.* Clonal neoantigens elicit T cell immunoreactivity and sensitivity to immune checkpoint blockade. *Science (1979)* **351**, 1463–1469 (2016).

82. Sato, Y. *et al.* CD4+ T cells induce rejection of urothelial tumors after immune checkpoint blockade. *JCI Insight* **3**, (2018).

83. Yi, M. *et al.* The role of neoantigen in immune checkpoint blockade therapy. *Experimental Hematology and Oncology* vol. 7 Preprint at https://doi.org/10.1186/s40164-018-0120-y (2018).

84. Caushi, J. X. *et al. Transcriptional Programs of Neoantigen-Specific TIL in Anti-PD-1-Treated Lung Cancers*. *Nature* vol. 596 (Springer US, 2021).

85. Kreiter, S. *et al.* Mutant MHC class II epitopes drive therapeutic immune responses to cancer. *Nature* **520**, 692–696 (2015).

86. Pardoll, D. M. The blockade of immune checkpoints in cancer immunotherapy. *Nature Reviews Cancer* vol. 12 252–264 Preprint at https://doi.org/10.1038/nrc3239 (2012).

87. Wei, S. C. *et al.* Distinct Cellular Mechanisms Underlie Anti-CTLA-4 and Anti-PD-1 Checkpoint Blockade. *Cell* **170**, 1120-1133.e17 (2017).

88. Yost, K. E. *et al.* Clonal replacement of tumor-specific T cells following PD-1 blockade. *Nat Med* **25**, 1251–1259 (2019).

89. Simpson, T. R. *et al.* Fc-dependent depletion of tumor-infiltrating regulatory t cells co-defines the efficacy of anti-CTLA-4 therapy against melanoma. *Journal of Experimental Medicine* **210**, 1695–1710 (2013).

90. Beavis, P. A. *et al.* Dual PD-1 and CTLA-4 Checkpoint blockade promotes antitumor immune responses through CD4 þ FOXP3 – cell–mediated modulation of CD103 þ dendritic cells. *Cancer Immunol Res* **6**, 1069–1081 (2018).

91. Selby, M. J. *et al.* Anti-CTLA-4 antibodies of IgG2a isotype enhance antitumor activity through reduction of intratumoral regulatory T cells. *Cancer Immunol Res* **1**, 32–42 (2013).

92. Bassez, A. *et al.* A single-cell map of intratumoral changes during anti-PD1 treatment of patients with breast cancer. *Nat Med* **27**, 820–832 (2021).

93. Yost, K. E. *et al.* Clonal replacement of tumor-specific T cells following PD-1 blockade. *Nat Med* **25**, 1251–1259 (2019).

94. Sharma, A. *et al.* Anti-CTLA-4 immunotherapy does not deplete Foxp3 þ regulatory T cells (Tregs) in human cancers. *Clinical Cancer Research* **25**, 1233–1238 (2019).

95. Yang, R. K. *et al. Identification of Biomarkers of Immune Checkpoint Blockade Efficacy in Recurrent or Refractory Solid Tumor Malignancies*. *Oncotarget* vol. 11 www.oncotarget.com (2020).

96. Ng Tang, D. *et al.* Increased frequency of ICOS+ CD4 T cells as a pharmacodynamic biomarker for anti-CTLA-4 therapy. *Cancer Immunol Res* **1**, 229–234 (2013).

97. Li, S. & Newell, E. Characterization of neoantigen-specific T cells in cancer resistant to immune checkpoint therapies. Preprint at (2021).

98. Liu, D., Jenkins, R. W. & Sullivan, R. J. Mechanisms of Resistance to Immune Checkpoint Blockade. *Am J Clin Dermatol* **20**, 41–54 (2019).

99. Fares, C. M., Van Allen, E. M., Drake, C. G., Allison, J. P. & Hu-Lieskovan, S. Mechanisms of Resistance to Immune Checkpoint Blockade: Why Does Checkpoint Inhibitor Immunotherapy Not Work for All Patients? *American Society of Clinical Oncology Educational Book* 147–164 (2019) doi:10.1200/edbk_240837.

100. Peng, M. *et al.* Neoantigen vaccine: An emerging tumor immunotherapy. *Molecular Cancer* vol. 18 Preprint at https://doi.org/10.1186/s12943-019-1055-6 (2019).

101. Sellars, M. C., Wu, C. J. & Fritsch, E. F. ll Cancer vaccines : Building a bridge over troubled waters. *Cell* 1–19 (2022) doi:10.1016/j.cell.2022.06.035.

102. Biswas, N., Chakrabarti, S., Padul, V., Jones, L. D. & Ashili, S. Designing neoantigen cancer vaccines, trials, and outcomes. *Frontiers in Immunology* vol. 14 Preprint at https://doi.org/10.3389/fimmu.2023.1105420 (2023).

103. Huff, A. L. *et al.* CD4 T cell–activating neoantigens enhance personalized cancer vaccine efficacy. *JCI Insight* **8**, (2023).

104. Provine, N. M. *et al.* Immediate Dysfunction of Vaccine-Elicited CD8 $^{+}$ T Cells Primed in the Absence of CD4 $^{+}$ T Cells. *The Journal of Immunology* **197**, 1809–1822 (2016).

105. Swartz, A. M. *et al.* A conjoined universal helper epitope can unveil antitumor effects of a neoantigen vaccine targeting an MHC class I-restricted neoepitope. *NPJ Vaccines* **6**, (2021).

106. Hung, C. F., Tsai, Y. C., He, L. & Wu, T. C. DNA vaccines encoding Ii-PADRE generates potent PADRE-specific CD4+ t-cell immune responses and enhances vaccine potency. *Molecular Therapy* **15**, 1211–1219 (2007).

107. Kumai, T. *et al.* Optimization of peptide vaccines to induce robust antitumor CD4 T-cell responses. *Cancer Immunol Res* **5**, 72–83 (2017).

108. Dorta-Estremera, S. *et al.* Mucosal HPV E6/E7 peptide vaccination in combination with immune checkpoint modulation induces regression of HPV þ oral cancers. *Cancer Res* **78**, 5327–5339 (2018).

109. Yang, S. F. *et al.* Neoantigen vaccination augments antitumor effects of anti-PD-1 on mouse hepatocellular carcinoma. *Cancer Lett* **563**, (2023).

110. Liu, L. *et al.* Concurrent delivery of immune checkpoint blockade modulates T cell dynamics to enhance neoantigen vaccine-generated antitumor immunity. *Nat Cancer* **3**, 437–452 (2022).

111. Ott, P. A. *et al.* A Phase Ib Trial of Personalized Neoantigen Therapy Plus Anti-PD-1 in Patients with Advanced Melanoma, Non-small Cell Lung Cancer, or Bladder Cancer. *Cell* **183**, 347-362.e24 (2020).

112. Coxon, A. T., Johanns, T. M. & Dunn, G. P. *An Innovative Immunotherapy Vaccine with Combination Checkpoint Blockade as a First Line Treatment for Glioblastoma in the Context of Current Treatments*.

113. Hu, Z. *et al.* Personal neoantigen vaccines induce persistent memory T cell responses and epitope spreading in patients with melanoma. *Nat Med* **27**, 515–525 (2021).

114. Rohaan, M. W., Wilgenhof, S. & Haanen, J. B. A. G. Adoptive cellular therapies: the current landscape. *Virchows Archiv* vol. 474 449–461 Preprint at https://doi.org/10.1007/s00428-018-2484-0 (2019).

115. Morotti, M. *et al.* Promises and challenges of adoptive T-cell therapies for solid tumours. *British Journal of Cancer* vol. 124 1759–1776 Preprint at https://doi.org/10.1038/s41416-021-01353-6 (2021).

116. Leko, V. *et al.* Identification of Neoantigen-Reactive Tumor-Infiltrating Lymphocytes in Primary Bladder Cancer. (2019) doi:10.4049/jimmunol.1801022.

117. Andersen, R. *et al.* Long-Lasting complete responses in patients with metastatic melanoma after adoptive cell therapy with tumor-infiltrating lymphocytes and an attenuated il2 regimen. *Clinical Cancer Research* **22**, 3734–3745 (2016).

118. Tucker, C. G. *et al.* Adoptive T Cell Therapy with IL-12–Preconditioned Low-Avidity T Cells Prevents Exhaustion and Results in Enhanced T Cell Activation, Enhanced Tumor Clearance, and Decreased Risk for Autoimmunity. *The Journal of Immunology* **205**, 1449–1460 (2020).

119. Lee, H. J. *et al. Expansion of Tumor-Infiltrating Lymphocytes and Their Potential for Application as Adoptive Cell Transfer Therapy in Human Breast Cancer*. vol. 8 www.impactjournals.com/oncotarget (2017).

120. Hall, M. L. *et al.* Expansion of tumor-infiltrating lymphocytes (TIL) from human pancreatic tumors. *J Immunother Cancer* **4**, (2016).

121. Rohaan, M. W., Van Den Berg, J. H., Kvistborg, P. & Haanen, J. B. A. G. Adoptive transfer of tumor-infiltrating lymphocytes in melanoma: A viable treatment option. *Journal for ImmunoTherapy of Cancer* vol. 6 Preprint at https://doi.org/10.1186/s40425-018-0391-1 (2018).

122. Rosenberg, S. A. *et al.* Durable complete responses in heavily pretreated patients with metastatic melanoma using T-cell transfer immunotherapy. *Clinical Cancer Research* **17**, 4550–4557 (2011).

123. Stevanović, S. *et al.* Complete regression of metastatic cervical cancer after treatment with human papillomavirus-targeted tumor-infiltrating T cells. *Journal of Clinical Oncology* **33**, 1543–1550 (2015).

124. Dafni, U. *et al.* Efficacy of adoptive therapy with tumor-infiltrating lymphocytes and recombinant interleukin-2 in advanced cutaneous melanoma: A systematic review and meta-analysis. *Annals of Oncology* vol. 30 1902–1913 Preprint at https://doi.org/10.1093/annonc/mdz398 (2019).

125. Rosenberg, S. A. & Restifo, N. P. Adoptive cell transfer as personalized immunotherapy for human cancer. *Science* vol. 348 62–68 Preprint at https://doi.org/10.1126/science.aaa4967 (2015).

126. Draper, L. M. *et al.* Targeting of HPV-16+ epithelial cancer cells by TCR gene engineered T cells directed against E6. *Clinical Cancer Research* **21**, 4431–4439 (2015).

127. Sheykhhasan, M., Manoochehri, H. & Dama, P. Use of CAR T-cell for acute lymphoblastic leukemia (ALL) treatment: a review study. *Cancer Gene Therapy* vol. 29 1080–1096 Preprint at https://doi.org/10.1038/s41417-021-00418-1 (2022).

128. June, C. H., O'connor, R. S., Kawalekar, O. U., Ghassemi, S. & Milone, M. C. *CAR T Cell Immunotherapy for Human Cancer*. https://www.science.org.

129. Brentjens, R. J. *et al.* CD19-targeted T cells rapidly induce molecular remissions in adults with chemotherapy-refractory acute lymphoblastic leukemia. *Sci Transl Med* **5**, (2013).

130. Lee, D. W. *et al.* T cells expressing CD19 chimeric antigen receptors for acute lymphoblastic leukaemia in children and young adults: A phase 1 dose-escalation trial. *The Lancet* **385**, 517–528 (2015).

131. Sadelain, M., Rivière, I. & Riddell, S. Therapeutic T cell engineering. *Nature* vol. 545 423–431 Preprint at https://doi.org/10.1038/nature22395 (2017).

132. Yee, C. *et al. Adoptive T Cell Therapy Using Antigen-Specific CD8 T Cell Clones for the Treatment of Patients with Metastatic Melanoma: In Vivo Persistence,*

Migration, and Antitumor Effect of Transferred T Cells. www.pnas.orgcgidoi10.1073pnas.242600099.

133. Morgan, R. A. *et al.* Cancer regression and neurological toxicity following anti-MAGE-A3 TCR gene therapy. *Journal of Immunotherapy* **36**, 133–151 (2013).

134. Robbins, P. F. *et al.* Tumor regression in patients with metastatic synovial cell sarcoma and melanoma using genetically engineered lymphocytes reactive with NY-ESO-1. *Journal of Clinical Oncology* **29**, 917–924 (2011).

135. Johnson, L. A. *et al.* Gene therapy with human and mouse T-cell receptors mediates cancer regression and targets normal tissues expressing cognate antigen. *Blood* **114**, 535–546 (2009).

136. Turtle, C. J. *et al.* Immunotherapy of non-Hodgkin's lymphoma with a defined ratio of CD8+ and CD4+ CD19-specific chimeric antigen receptor-modified T cells. *Sci Transl Med* **8**, (2016).

137. Klebanoff, C. A. *et al. Central Memory Selftumor-Reactive CD8 T Cells Confer Superior Antitumor Immunity Compared with Effector Memory T Cells*. www.pnas.orgcgidoi10.1073pnas.0503726102.

138. Cha, E., Graham, L., Manjili, M. H. & Bear, H. D. IL-7 + IL-15 are superior to IL-2 for the ex vivo expansion of 4T1 mammary carcinoma-specific T cells with greater efficacy against tumors in vivo. *Breast Cancer Res Treat* **122**, 359–369 (2010).

139. Gomez-Eerland, R. *et al.* Manufacture of Gene-Modified Human T-Cells with a Memory Stem/Central Memory Phenotype. *Hum Gene Ther Methods* **25**, 277–287 (2014).

140. Lai, J. *et al.* Adoptive cellular therapy with T cells expressing the dendritic cell growth factor Flt3L drives epitope spreading and antitumor immunity. *Nat Immunol* **21**, 914–926 (2020).

141. Conde, E. *et al.* Epitope spreading driven by the joint action of CART cells and pharmacological STING stimulation counteracts tumor escape via antigen-loss variants. *J Immunother Cancer* **9**, (2021).

142. Heckler, M. & Dougan, S. K. Unmasking Pancreatic Cancer: Epitope Spreading After Single Antigen Chimeric Antigen Receptor T-Cell Therapy in a Human Phase I Trial. *Gastroenterology* vol. 155 11–14 Preprint at https://doi.org/10.1053/j.gastro.2018.06.023 (2018).

143. Dolina, J. S. *et al.* Linked CD4+/CD8+ T cell neoantigen vaccination overcomes immune checkpoint blockade resistance and enables tumor regression. *Journal of Clinical Investigation* **133**, (2023).

144. Hemmer, B. *et al. Minimal Peptide Length Requirements for CD4 T Cell Clones-Implications for Molecular Mimicry and T Cell Survival*. *International Immunology* vol. 12 www.expasy.ch/sprot/scnpsit2.html (2000).

145. Oliveira, G. *et al.* Phenotype, specificity and avidity of antitumour CD8+ T cells in melanoma. *Nature* **596**, 119–125 (2021).

146. Stone, J. D. & Kranz, D. M. Role of T cell receptor affinity in the efficacy and specificity of adoptive T cell therapies. *Frontiers in Immunology* vol. 4 Preprint at https://doi.org/10.3389/fimmu.2013.00244 (2013).